

Facially Coordinating Triamine Ligands with a Cyclic Backbone: Some Structure–Stability Correlations[†]

Christian Neis, David Petry, Alexandre Demangeon, Bernd Morgenstern, Dirk Kuppert, Jochen Huppert, Stefan Stucky, and Kaspar Hegetschweiler*

Anorganische Chemie, Universität des Saarlandes, Postfach 15 11 50, D-66041 Saarbrücken, Germany

Received July 12, 2010

Metal complex formation of the two cyclic triamines 6-methyl-1,4-diazepan-6-amine (MeL^a) and all-*cis*-2,4,6-trimethylcyclohexane-1,3,5-triamine (Me₃tach) was studied. The structure of the free ligands (H_xMeL^a)^{x+} and H_xMe₃tach^{x+} (0 ≤ x ≤ 3) was investigated by pH-dependent NMR spectroscopy and X-ray diffraction experiments. The crystal structure of (H₂Me₃tach)(*p*-O₃S–C₆H₄–CH₃)₂ showed a chair conformation with axial nitrogen atoms for the doubly protonated species. In contrast to a previous report, Me₃tach was found to be a stronger base than the parent *cis*-cyclohexane-1,3,5-triamine (tach); p*K*_a-values of H₃Me₃tach³⁺ (25 °C, 0.1 M KCl): 5.2, 7.4, 11.2. The crystal structures of (H₃MeL^a)(BiCl₆)·2H₂O and (H₃MeL^a)(ClO₄)Cl₂ exhibited two distinct twisted chair conformations of the seven membered diazepane ring. [Co(MeL^a)₂]³⁺ (*cis*: **1**³⁺, *trans*: **2**³⁺), *trans*-[Fe(MeL^a)₂]³⁺ (**3**³⁺), [(MeL^a)ClCd(μ₂-Cl)]₂ (**4**), *trans*-[Cu(MeL^a)₂]²⁺ (**5**²⁺), and [Cu(HMeL^a)Br₃] (**6**) were characterized by single crystal X-ray analysis of **1**(ClO₄)₃·H₂O, **2**Br₃·H₂O, **3**(ClO₄)₃·0.8MeCN·0.2MeOH, **4**, **5**Br₂·0.5MeOH, and **6**·H₂O. Formation constants and redox potentials of MeL^a complexes were determined by potentiometric, spectrophotometric, and cyclovoltammetric measurements. The stability of [M^{II}(MeL^a)₂]²⁺-complexes is low. In comparison to the parent 1,4-diazepan-6-amine (L^a), it is only slightly enhanced. In analogy to L^a, MeL^a exhibited a pronounced tendency for forming protonated species such as [M^{II}(HMeL^a)₂]³⁺ or [M^{II}(MeL^a)(HMeL^a)]³⁺ (see **6** as an example). In contrast to MeL^a, Me₃tach forms [M^{II}L]²⁺ complexes (M = Cu, Zn) of very high stability, and the coordination behavior corresponds mainly to an “all-or-nothing” process. Molecular mechanics calculations showed that the low stability of L^a and MeL^a complexes is mainly due to a large amount of torsional strain within the pure chair conformation of the diazepane ring, required for tridentate coordination. This behavior is quite contrary to Me₃tach and tacn (tacn = 1,4,7-triazacyclononane), where the main portion of strain is already preformed in the free ligand, and the amount, generated upon complex formation, is comparably low.

Introduction

With their restriction to facial coordination, cyclic triamines such as *cis*-cyclohexane-1,3,5-triamine (tach) or 1,4,7-triazacyclononane (tacn) are well established building blocks for the construction of catalytically active metal complexes or for modeling the active site of metalloenzymes.^{1–3} On the basis of the limited conformational flexibility of the ligand

backbone, these triamines afford a donor set with a comparably well-defined geometry and thus, at least to a certain extent, predictability of structure, stability, and reactivity. Tach and tacn have been well-known for many years; they are distinguished by providing exclusively either exocyclic (primary) or endocyclic (secondary) nitrogen donors for

[†] Facially Coordinating Cyclic Triamines, 5. – Part 4: Reference 21.

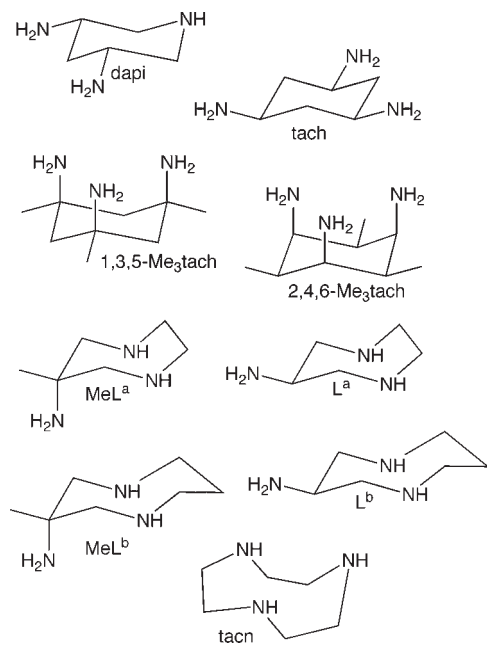
*To whom correspondence should be addressed. Phone: (+49)-681-3022715. Fax: (+49)-681-3022663. E-mail: hegetschweiler@mx.uni-saarland.de.

(1) (a) Pecoraro, V. L.; Hsieh, W.-Y. *Met. Ions Biol. Syst.* **2000**, 37, 429. (b) Dube, C. E.; Mukhopadhyay, S.; Bonitatebus, P. J.; Staples, R. J.; Armstrong, W. H. *Inorg. Chem.* **2005**, 44, 5161.

(2) (a) Boseggia, E.; Gatos, M.; Lucatello, L.; Mancin, F.; Moro, S.; Palumbo, M.; Sissi, C.; Tecilla, P.; Tonellato, U.; Zagotto, G. *J. Am. Chem. Soc.* **2004**, 126, 4543. (b) Lewis, E. A.; Khodr, H. H.; Hider, R. C.; Lindsay Smith, J. R.; Walton, P. H. *Dalton Trans.* **2004**, 187. (c) Nairn, A. K.; Archibald, S. J.; Bhalla, R.; Gilbert, B. C.; MacLean, E. J.; Teat, S. J.; Walton, P. H. *Dalton Trans.* **2006**, 172. (d) Kajita, Y.; Arai, H.; Saito, T.; Saito, Y.; Nagatomo, S.; Kitagawa, T.; Funahashi, Y.; Ozawa, T.; Masuda, H. *Inorg. Chem.* **2007**, 46, 3322.

(3) (a) Fry, F. H.; Fischmann, A. J.; Belousoff, M. J.; Spiccia, L.; Brügger, J. *Inorg. Chem.* **2005**, 44, 941. (b) Sibbons, K. F.; Shastri, K.; Watkinson, M. *Dalton Trans.* **2006**, 645. (c) Hage, R.; Lienke, A. *J. Mol. Catal. A: Chem.* **2006**, 251, 150. (d) Lindsay Smith, J. R.; Gilbert, B. C.; Mairata i Payeras, A.; Murray, J.; Lowdon, T. R.; Oakes, J.; Pons i Prats, R.; Walton, P. H. *J. Mol. Catal. A: Chem.* **2006**, 251, 114. (e) de Boer, J. W.; Browne, W. R.; Brinksma, J.; Alsters, P. L.; Hage, R.; Feringa, B. L. *Inorg. Chem.* **2007**, 46, 6353. (f) Romakh, V. B.; Therrien, B.; Süß-Fink, G.; Shul'pin, G. B. *Inorg. Chem.* **2007**, 46, 3166. (g) Scarpellini, M.; Gätjens, J.; Martin, O. J.; Kampf, J. W.; Sherman, S. E.; Pecoraro, V. L. *Inorg. Chem.* **2008**, 47, 3584. (h) Bodsgard, B. R.; Clark, R. W.; Ehrbar, A. W.; Burstyn, J. N. *Dalton Trans.* **2009**, 2365.

(4) (a) Chaudhuri, P.; Wieghardt, K. *Prog. Inorg. Chem.* **1987**, 35, 329. (b) Moreland, A. C.; Rauchfuss, T. B. *J. Am. Chem. Soc.* **1998**, 120, 9376. (c) Slep, L. D.; Mijovilovich, A.; Meyer-Klaucke, W.; Weyhermüller, T.; Bill, E.; Bothe, E.; Neese, F.; Wieghardt, K. *J. Am. Chem. Soc.* **2003**, 125, 15554.

Chart 1. Structural Representations and Abbreviations for Some Selected Cyclic Triamine Ligands

metal binding (Chart 1).^{4,5} More recently, the coordination chemistry of *cis*-3,4-diamino-pyrrolidine,⁶ *cis*-3,5-diaminopiperidine (dapi),⁷ and 1,4-diazepan-6-amine (L^a),^{8–10} carrying both, endocyclic and exocyclic nitrogen donors, have been investigated. The different reactivity of the primary and secondary amino groups opens new routes to a selective derivatization, rendering such intermediate types particularly versatile.^{6,8}

In a recent paper,⁸ entitled “*First-Transition-Metal Complexes Containing the Ligands 6-Amino-6-methylperhydro-1,4-diazepine (AAZ) and a New Functionalized Derivative: Can AAZ Act as a Mimetic Ligand for 1,4,7-Triazacyclononane?*”, arguments were provided for using diazepane-based triamines as a promising source for new tailored metal-complexing agents. In our own research program, we discovered, however, that metal complexes of L^a with divalent

transition metal cations are of surprisingly low stability.¹⁰ This is in contrast to tacn, which forms exceptionally stable complexes.¹¹ A possible explanation for this finding is the equatorial (“wrong”) orientation of the amino group in the most stable conformation of L^a. In the methylated derivative MeL^a (6-methyl-1,4-diazepan-6-amine, denoted as AAZ in the above-mentioned paper),⁸ an axial orientation of the amino group, as required for complex formation, is expected to be more readily accessible, and in terms of a better pre-orientation of the donor set, complex formation should thus be favored.

A similar situation is observed for tach,¹² where the conformation required for a tris-chelate formation is strongly disfavored because of 1,3-diaxial repulsion. Derivatives with additional substituents in a suitable position would stabilize a conformation with axial amino groups, and with regard to better preorientation, one could again expect formation of complexes of higher stability. Two corresponding trimethylated derivatives, all-*cis*-2,4,6-trimethylcyclohexane-1,3,5-triamine (2,4,6-Me₃tach)¹³ and *cis*-1,3,5-trimethylcyclohexane-1,3,5-triamine (1,3,5-Me₃tach)¹⁴ have been described. Unfortunately, the stability of their metal complexes has not yet been reported. For 1,3,5-triamino-1,3,5-trideoxy-*cis*-inositol (taci)¹⁵ and its *O*-methylated derivative (tmca),¹⁶ metal complexes of increased stability have indeed been observed. It is, however, well-known that a hydroxy or methoxy group is sterically less demanding than an amino group, and a conformation with equatorial amino groups is still predominant for taci and tmca in their free (neutral) form in H₂O.¹⁶ Methyl groups are sterically more demanding than hydroxy or methoxy groups, and the donor set of the trimethylated derivatives should be even better preorganized.

For a better understanding of such preorientation effects, it would be helpful to compare the tach and L^a complexes directly with corresponding counterparts of the methylated derivatives. In this contribution we will analyze the coordination behavior of the diazepane based ligands L^a and MeL^a, and the following topics will explicitly be addressed: what are the specific characteristics of the diazepane based ligands in comparison to the cyclohexane-based tach and the macrocyclic tacn? Are these characteristics of relevance when discussing L^a or MeL^a as substitutes for tacn? What is the impact of adding methyl groups to the ligand backbone? Is there really such an effect as “higher stability by better pre-orientation of the donor set”? Is it in general possible to rationalize the observed differences in a conclusive manner in terms of the steric prerequisites of the ligands? To answer these questions, we investigated the coordination behavior of MeL^a by means of structure analysis in the solid state and equilibrium studies in solution. In addition we performed

(5) (a) Childers, R. F.; Wentworth, R. A. D.; Zompa, L. J. *Inorg. Chem.* **1971**, *10*, 302. (b) Ammeter, J. H.; Bürgi, H. B.; Gamp, E.; Meyer-Sandrin, V.; Jensen, W. P. *Inorg. Chem.* **1979**, *18*, 733. (c) Fabbrizzi, L.; Micheloni, M.; Paoletti, P. *J. Chem. Soc., Dalton Trans.* **1980**, 1055. (d) Schwarzenbach, G.; Bürgi, H.-B.; Jensen, W. P.; Lawrance, G. A.; Monsted, L.; Sargeson, A. M. *Inorg. Chem.* **1983**, *22*, 4029. (e) Brand, U.; Vahrenkamp, H. *Inorg. Chim. Acta* **1992**, *198–200*, 663.

(6) Kuppert, D.; Sander, J.; Roth, C.; Wörle, M.; Weyhermüller, T.; Reiss, G. J.; Schilde, U.; Müller, I.; Hegetschweiler, K. *Eur. J. Inorg. Chem.* **2001**, 2525.

(7) Pauly, J. W.; Sander, J.; Kuppert, D.; Winter, M.; Reiss, G. J.; Zürcher, F.; Hoffmann, R.; Fässler, T. F.; Hegetschweiler, K. *Chem.—Eur. J.* **2000**, *6*, 2830.

(8) Peralta, R. A.; Neves, A.; Bortoluzzi, A. J.; Casellato, A.; dos Anjos, A.; Greatti, A.; Xavier, F. R.; Szpoganicz, B. *Inorg. Chem.* **2005**, *44*, 7690.

(9) (a) Aime, S.; Calabi, L.; Cavallotti, C.; Gianolio, E.; Giovenzana, G. B.; Losi, P.; Maiocchi, A.; Palmisano, G.; Sisti, M. *Inorg. Chem.* **2004**, *43*, 7588. (b) Rey, N. A.; Neves, A.; Bortoluzzi, A. J.; Pich, C. T.; Terenzi, H. *Inorg. Chem.* **2007**, *46*, 348. (c) Rey, N. A.; Neves, A.; Silva, P. P.; Paula, F. C. S.; Silveira, J. N.; Botelho, F. V.; Vieira, L. Q.; Pich, C. T.; Terenzi, H.; Pereira-Maia, E. C. *J. Inorg. Biochem.* **2009**, *103*, 1323. (d) Elemento, E. M.; Parker, D.; Aime, S.; Gianolio, E.; Lattuada, L. *Org. Biomol. Chem.* **2009**, *7*, 1120. (e) Comba, P.; Haaf, C.; Wadepohl, H. *Inorg. Chem.* **2009**, *48*, 6604. (f) Comba, P.; Haaf, C.; Lienke, A.; Muruganatham, A.; Wadepohl, H. *Chem.—Eur. J.* **2009**, *15*, 10880.

(10) Romba, J.; Kuppert, D.; Morgenstern, B.; Neis, C.; Steinhäuser, S.; Weyhermüller, T.; Hegetschweiler, K. *Eur. J. Inorg. Chem.* **2006**, 314.

(11) Yang, R.; Zompa, L. J. *Inorg. Chem.* **1976**, *15*, 1499.

(12) Fabbrizzi, L.; Micheloni, M.; Paoletti, P. *Inorg. Chem.* **1976**, *15*, 1451.

(13) (a) de Angelis, S.; Batsanov, A.; Norman, T. J.; Parker, D.; Senanayake, K.; Vepsäläinen, J. *J. Chem. Soc., Chem. Commun.* **1995**, 2361. (b) Parker, D.; Senanayake, K.; Vepsäläinen, J.; Williams, S.; Batsanov, A. S.; Howard, J. A. K. *J. Chem. Soc., Perkin Trans. 2* **1997**, 1445.

(14) (a) Menger, F. M.; Bian, J.; Azov, V. A. *Angew. Chem., Int. Ed.* **2002**, *41*, 2581. (b) Regino, C. A. S.; Torti, S. V.; Ma, R.; Yap, G. P. A.; Kreisel, K. A.; Torti, F. M.; Planalp, R. P.; Brechbiel, M. W. *J. Med. Chem.* **2005**, *48*, 7993.

(15) Ghisletta, M.; Hausherr-Primo, L.; Gajda-Schranz, K.; Machula, G.; Nagy, L.; Schmalle, H. W.; Rihs, G.; Endres, F.; Hegetschweiler, K. *Inorg. Chem.* **1998**, *37*, 997.

(16) Weber, M.; Kuppert, D.; Hegetschweiler, K.; Gramlich, V. *Inorg. Chem.* **1999**, *38*, 859.

molecular mechanics calculations to locate specific steric effects in the complexes formed. Since the formation constants of 2,4,6-Me₃tach-complexes are unknown, we also prepared this triamine and investigated its structure, basicity and complex formation with Cu²⁺ and Zn²⁺ in solution.

Experimental Section

Materials and Instrumentation. The chemicals used for the synthetic work were of reagent grade quality and were used as obtained. Dowex 50 W-X2 (100–200 mesh, H⁺ form) and Dowex 2-X8 (50–100 mesh, Cl⁻ form) were from Fluka. The anion resin was converted into the OH⁻ form using 0.3 M aqueous NaOH. UV/vis spectra of the Co^{III} and Fe^{III} complexes were measured on a Uvikon 941 spectrophotometer (H₂O, 25 ± 3 °C). IR spectra were recorded on a Bruker Vector 22 FT IR spectrometer equipped with a Golden Gate ATR unit. ¹H and ¹³C{¹H} NMR spectra were measured in D₂O (294 K, Bruker DRX Avance 400 MHz NMR spectrometer, resonance frequencies: 400.13 MHz for ¹H and 100.6 MHz for ¹³C). Chemical shifts are given in ppm relative to D₄-sodium (trimethylsilyl)propionate as internal standard (δ = 0 ppm). The pH* of each sample¹⁷ was adjusted using appropriate solutions of DCl and NaOD in D₂O. 2D spectra were measured as gradient-selected ¹H–¹³C HMBP experiments.¹⁸

H₃Me₃tach(SO₄)_{1.5}·3H₂O¹⁹. H₃Me₃tach(SO₄)_{1.5}·3H₂O was prepared following the protocol given by Parker et al.¹³ with some minor modifications. The hydrogenation of the aromatic precursor (22 °C, 3 bar H₂ pressure, 2.5 h, in aqueous H₂SO₄) was performed using a Rh–Pt-oxide-hydrate catalyst (45.6% Rh and 19.9% Pt).²⁰ ¹H NMR (D₂O, pH* < 2) δ 1.29 (d, *J* = 8 Hz, 9H), 2.67 (m, 3H), 3.77 (t, *J* = 5 Hz, 3H). ¹³C NMR (D₂O, pH* < 2) δ 12.3, 35.3, 54.8. Anal. Calcd (%) for C₉H₃₀N₃O₉S_{1.5} (372.45): C, 29.02; H, 8.12; N, 11.28. Found: C, 28.66; H, 8.08; N, 11.21.

H₃Me₃tachCl₃·0.7H₂O. H₃Me₃tach(SO₄)_{1.5}·3H₂O (1 g, 2.7 mmol) was dissolved in H₂O (50 mL) and sorbed on Dowex 50 W. The column was washed with H₂O (1 L) and eluted with 3 M aqueous HCl (500 mL). The eluate was evaporated to dryness, and the resulting white residue was dried in vacuo (710 mg, 90%). Anal. Calcd (%) for C₉H_{25.4}Cl₃N₃O_{0.7} (293.28): C, 36.86; H, 8.73; N, 14.33. Found: C, 36.86; H, 8.48; N, 14.40.

H₂Me₃tach(*p*-toluenesulfonate)₂. H₃Me₃tach(SO₄)_{1.5}·3H₂O (1 g, 2.7 mmol) was dissolved in H₂O and deprotonated on Dowex 2 (OH⁻ form). The eluate was evaporated to dryness under reduced pressure. *p*-Toluenesulfonic acid monohydrate (1 g, 5.3 mmol) dissolved in EtOH (25 mL) was added to the resulting residue. The solution was stored for several days at 4 °C, yielding white crystals, suitable for X-ray structural analysis. Anal. Calcd (%) for C₂₃H₃₇N₃O₆S₂ (515.69): C, 53.57; H, 7.23; N, 8.15. Found: C, 53.51; H, 7.08; N, 7.87.

(17) In this paper, the term pH* refers to the direct pH-meter reading (Metrohm 713 pH meter) of the D₂O samples, using a Metrohm glass electrode with an aqueous (H₂O) Ag/AgCl-reference that was calibrated with aqueous (H₂O) buffer solutions. For the interconversion of pH* and pD see: Alderighi, L.; Bianchi, A.; Biondi, L.; Calabi, L.; De Miranda, M.; Gans, P.; Ghelli, S.; Losi, P.; Paleari, L.; Sabatini, A.; Vacca, A. *J. Chem. Soc., Perkin Trans. 2* **1999**, 2741.

(18) (a) Hurd, R. E. *J. Magn. Reson.* **1990**, *87*, 422. (b) von Kienlin, M.; Moonen, C. T. W.; van der Toorn, A.; van Zijl, P. C. M. *J. Magn. Reson.* **1991**, *93*, 423. (c) Hurd, R. E.; John, B. K. *J. Magn. Reson.* **1991**, *91*, 648. (d) Ruiz-Cabello, J.; Vuister, G. W.; Moonen, C. T. W.; van Gelderen, P.; Cohen, J. S.; van Zijl, P. C. M. *J. Magn. Reson.* **1992**, *100*, 282. (e) Willker, W.; Leibfritz, D.; Kerssebaum, R.; Bermel, W. *Magn. Reson. Chem.* **1993**, *31*, 287.

(19) In this paper, the simple acronym Me₃tach generally refers to all-*cis*-2,4,6-trimethyl-cyclohexane-1,3,5-triamine. An explicit listing of the positions of the methyl groups, i.e., 2,4,6-Me₃tach (or 1,3,5-Me₃tach for Menger's compound) is only given, if such a specification is required by context.

(20) (a) Nishimura, S. *Bull. Chem. Soc. Jpn.* **1960**, *33*, 566. (b) Nishimura, S. *Bull. Chem. Soc. Jpn.* **1961**, *34*, 1544.

MeL^a. MeL^a was prepared, following the protocol of Aime et al.^{9a} As reported, the free triamine is a colorless oil. It is sensitive to CO₂.²¹ For a convenient handling, it was transformed into the hydrochloride MeL^a·3HCl·0.33H₂O or into the hydrobromide MeL^a·3HBr·H₂O. Anal. Calcd (%) for C₆H₁₈Cl₃N₃·0.33H₂O (244.53): C, 29.46; H, 7.69; N, 17.18. Found: C, 29.84; H, 7.76; N, 16.91. Anal. Calcd (%) for C₆H₁₈Br₃N₃·H₂O (389.95): C, 18.48; H, 5.17; N, 10.78. Found: C, 18.70; H, 5.17; N, 10.74.

(H₃MeL^a)(BiCl₆)·2H₂O. MeL^a·3HCl·0.33H₂O (49 mg, 0.20 mmol) was dissolved in H₂O (10 mL). To this solution was added Bi(NO₃)₃·5H₂O (97 mg, 0.20 mmol) and hydrochloric acid (6 M, 1 mL) up to pH < 1. The solution was allowed to evaporate slowly at ambient conditions, yielding single crystals, suitable for X-ray structural analysis. Anal. Calcd (%) for C₆H₁₈BiCl₆N₃·2H₂O (589.96): C, 12.22; H, 3.76; N, 7.12. Found: C, 12.41; H, 3.70; N, 7.11. A part of the crystals was removed and dried under reduced pressure. Anal. Calcd (%) for the monohydrate C₆H₁₈BiCl₆N₃·H₂O (571.94): C, 12.60; H, 3.52; N, 7.34. Found: C, 12.84; H, 3.45; N, 7.55. IR (cm⁻¹): 849, 956, 1092, 1237, 1397, 1445, 1508, 1565, 2958, 3480.

(H₃MeL^a)(ClO₄)Cl₂. MeL^a·3HCl·0.33H₂O (49 mg, 0.20 mmol) was dissolved in H₂O (10 mL). Concentrated hydrous HClO₄ (70%, 0.5 mL) was added. The solution was allowed to evaporate slowly at ambient conditions, yielding colorless crystals, suitable for X-ray structural analysis. Anal. Calcd (%) for C₆H₁₈Cl₃N₃O₄ (302.58): C, 23.82; H, 6.00; N, 13.89. Found: C, 23.38; H, 5.98; N, 13.62.

[Co(MeL^a)₂]Cl₃. MeL^a·3HCl·0.33H₂O (3.4 g, 14 mmol) was dissolved in H₂O (50 mL), and the pH of the solution was adjusted to 8 by adding NaOH (1 M). Solid CoCl₂·6H₂O (1.67 g, 7 mmol) was added, and the solution was aerated with oxygen under stirring for 24 h, yielding a red-orange solution. Chromatography on SP-Sephadex C-25 with trisodium citrate (0.2 M) yielded two major orange bands of the *cis* and *trans* isomer of [Co(MeL^a)₂]³⁺ (**1**³⁺ and **2**³⁺), respectively. The two fractions were desalted on Dowex 50 (3 M HCl) and evaporated to dryness.

1Cl₃·3.5H₂O. Yield: 19%. ¹H NMR (D₂O): δ 1.38 (s, 3H), 2.72 (m, 2H), 3.05 (m, 2H), 3.37 (m, 3H), 3.72 (m, 1H). ¹³C NMR (D₂O): δ 20.4, 55.8, 56.3, 64.7, 66.5, 66.8 ppm. IR (cm⁻¹): 572, 833, 979, 1006, 1068, 1142, 1229, 1304, 1361, 1455, 1588, 2358, 2861, 3029. UV/vis: λ_{max} (ε) = 342 nm (105), 472 nm (121). Anal. Calcd (%) for C₁₂H₃₀Cl₃CoN₆·3.5H₂O (486.75): C, 29.61; H, 7.66; N, 17.27. Found: C, 29.60; H, 7.56; N, 16.94.

2Cl₃·3.5H₂O. Yield: 40%. ¹H NMR (D₂O): δ 1.35 (s, 3H), 2.69 (d, *J* = 13 Hz, 2H), 2.90 (m, 2H), 3.46 (m, 2H), 3.53 (d, *J* = 13 Hz, 2H). ¹³C NMR (D₂O): δ 20.0, 55.6, 64.1, 66.9. IR (cm⁻¹): 573, 787, 819, 835, 914, 975, 1002, 1064, 1140, 1171, 1219, 1315, 1376, 1393, 1417, 1456, 1497, 1582, 1634, 2362, 3074 cm⁻¹. UV/vis: λ_{max} (ε) = 336 nm (66), 471 nm (69). Anal. Calcd (%) for C₁₂H₃₀Cl₃CoN₆·3.5H₂O (486.75): C, 29.61; H, 7.66; N, 17.27. Found: C, 30.08; H, 7.45; N, 17.03.

Growth of single crystals: The two isomeric complexes **1**Cl₃·3.5H₂O and **2**Cl₃·3.5H₂O were dissolved in H₂O. The solutions were acidified either with 70% hydrous HClO₄ (**1**³⁺) or concentrated hydrous HBr (**2**³⁺) up to pH < 1. Slow evaporation at ambient conditions yielded orange crystals of composition **1**(ClO₄)₃·H₂O²² and **2**Br₃·H₂O, respectively. Anal. Calcd (%) for C₁₂H₃₀Cl₃CoN₆O₁₂·H₂O (633.71): C, 22.74; H, 5.09; N, 13.26. Found: C, 22.85; H, 5.27; N, 12.95. IR (cm⁻¹): 559, 616 (br), 928, 978, 1000, 1049 (br), 1174, 1229, 1370, 1382, 1434, 1459, 1494, 1616, 2362, 3150, 3261, 3501 cm⁻¹. Anal. Calcd (%) for C₁₂H₃₀Br₃CoN₆·H₂O (575.07): C, 25.06; H, 5.61; N, 14.61. Found: C, 25.35; H, 5.83; N, 14.44. IR (cm⁻¹): 583, 783, 816,

(21) Neis, C.; Weyhermüller, T.; Bill, E.; Stucky, S.; Hegetschweiler, K. *Eur. J. Inorg. Chem.* **2008**, 1019.

(22) **Caution!** Organic perchlorate salts are potentially explosive.

833, 912, 974, 999, 1060, 1138, 1171, 1215, 1263, 1318, 1357, 1375, 1394, 1416, 1457, 1494, 1574, 1621, 2359, 2974, 3139.

[Fe(MeL^a)₂](ClO₄)₃·0.8MeCN·0.2MeOH.²² MeL^a·3HCl·0.33H₂O (95 mg, 0.39 mmol) was dissolved in H₂O and deprotonated on Dowex 2 (OH⁻ form). The solution was evaporated to dryness, and the resulting oil was dissolved in MeOH (3 mL). Fe(ClO₄)₃·H₂O (73 mg, 0.2 mmol), dissolved in MeCN (3 mL), was added. The resulting solution was placed in a desiccator together with a beaker with EtOAc. Red-orange crystals of [Fe(MeL^a)₂]³⁺ (3³⁺) as a perchlorate salt,²² suitable for X-ray diffraction, were obtained after a few days. UV/vis (MeCN): λ_{max} (ε) = 337 nm (sh, 280), 443 nm (78), 509 nm (sh, 43). IR (cm⁻¹): 620, 692, 761, 824, 928, 970, 1000, 1043 (br), 1220, 1370, 1426, 1465, 1494, 1588, 3254 (br). Anal. Calcd (%) for C₁₂H₃₀Cl₃FeN₆O₁₂·0.8MeCN·0.2MeOH (651.85): C, 25.43; H, 5.13; N, 14.61. Found: C, 25.86; H, 5.16; N, 14.39.

[Cd(MeL^a)Cl₂]₂·MeL^a·3HCl·0.33H₂O (122 mg, 0.50 mmol) was dissolved in H₂O and deprotonated on Dowex 2 (OH⁻ form). The solution was concentrated to a volume of 10 mL, and CdCl₂·2H₂O (55 mg, 0.25 mmol) was added. It was acidified with 0.1 M hydrous HClO₄ to pH ≈ 6, and was allowed to stand open to the air for a few days, yielding crystals of **4** suitable for X-ray structural analysis. IR (cm⁻¹): 623, 651, 762, 848, 895, 933, 995, 1028, 1052, 1129, 1149, 1330, 1377, 1461, 1586, 2858, 3269, 3321. Anal. Calcd (%) for C₁₂H₃₀Cd₂Cl₄N₆ (625.04): C, 23.06; H, 4.84; N, 13.45. Found: C, 23.10; H, 4.91; N, 13.00.

trans-[Cu(MeL^a)₂Br₂·0.5MeOH. To a MeOH solution (3 mL) of MeL^a (0.50 mmol), which was prepared as described above for 3³⁺, was added CuBr₂ (44 mg, 0.20 mmol) dissolved in MeCN (3 mL). The resulting solution was placed in a desiccator together with a beaker with EtOAc. After 3 days blue crystals of *trans*-[Cu(MeL^a)₂]²⁺ (5²⁺) as 5Br₂·0.5MeOH, suitable for X-ray structural analysis, deposited together with an additional unidentified colorless material.

[Cu(HMeL^a)Br₃]·H₂O. MeL^a·3HCl·0.33H₂O (95 mg, 0.39 mmol) was dissolved in H₂O and deprotonated on Dowex 2 (OH⁻ form). The solution was concentrated to a total volume of 8 mL, and CuBr₂ (87 mg, 0.39 mmol) was added. An aqueous 3 M HBr solution was added dropwise until pH ≈ 4. The solution was allowed to stand at ambient conditions open to the air, yielding green crystals of 6·H₂O suitable for X-ray structural analysis within a few days. IR (cm⁻¹): 597, 630, 869, 908, 924, 968, 999, 1040, 1082, 1102, 1153, 1238, 1314, 1379, 1409, 1432, 1455, 1584, 2800 (br), 3176, 3282, 3457, 3518. Anal. Calcd (%) for C₆H₁₆Br₃CuN₃·H₂O (451.49): C, 15.96; H, 4.02; N, 9.31. Found: C, 16.14; H, 4.32; N, 9.35.

NMR Titrations. An experimental setup was used as described previously.²³ Solutions of Me₃tach and MeL^a in 1 M DCl/D₂O were neutralized stepwise by adding small increments of a NaOD/D₂O solution (0.1 M). After each base addition, the pH* was measured,¹⁷ and a 0.6 mL aliquot was taken for the recording of a ¹H NMR spectrum. A total of 25 (Me₃tach) or 24 (MeL^a) spectra was recorded in the range of 0.03 < pH* < 12.42 and 0.77 < pH* < 12.1, respectively. Least squares calculations ∑(δ_{obs} - δ_{calcd})² = min were performed assuming a rapid equilibrium between the differently protonated species H_xL^{x+} (0 ≤ x ≤ 3), using the computer program NMR-Tit.²⁴

Cyclic Voltammetry. Cyclic voltammograms were recorded at ambient temperature (25 ± 2 °C) using a BAS C2 cell combined with a BAS 100B/W2 potentiostat or a Metrohm VA Computrace 797 potentiostat, a Hg (for the Co-complex) or Pt (for the Fe- and Ni-complexes) working electrode, a Pt counter electrode, and a Ag/AgCl reference electrode. Samples of the Co-MeL^a-system (0.5 M KCl) were prepared using solid 2Cl₃·

3.5H₂O. The total Co concentration was 5 mM, and the pH was adjusted to 6.6. Samples of the Fe- and Ni-MeL^a systems (0.5 M KCl) were prepared in situ using FeSO₄·7H₂O or NiSO₄·6H₂O and MeL^a·3HCl·0.33H₂O (total metal = 5 mM, total MeL^a = 10 mM). The pH was adjusted to 7.4 or 7.1, respectively. Fe-dapi samples (dapi = *cis*-3,5-diamino-piperidine) were also prepared in situ using FeSO₄·7H₂O and dapi·3HCl⁷ (total Fe = 10 mM, total dapi = 20 mM, 1 M KNO₃, pH = 8.0).

Potentiometric and Spectrophotometric Measurements. The experimental setup has already been described.²⁵ All titrations were performed at 25.0 °C under an atmosphere of N₂ or Ar, scrubbed with a solution of the inert electrolyte. The electrode was checked by calibration titrations prior to, and after, each measurement, and the data was only considered if ΔE° < 1 mV. In accordance with the ionic strength of the sample solutions, 0.10 M KOH and 0.10 M HCl or 0.10 M HNO₃ (for 0.1 M KCl or KNO₃), or 1.0 M KOH and 1.0 M HCl or 1.0 M HNO₃ (for 1.0 M KCl or KNO₃) were used as titrants (Merck Titrisol). H₂O was distilled twice (quartz apparatus). Stock solutions of suitable metal salts (Merck Titrisol) were used for sample preparation. The protonated ligands were applied as solid hydrochlorides. Their purity was checked by C,H,N analysis and ¹H NMR spectroscopy. Note that stock solutions of the hydrochlorides cannot be stored over a longer period because of microbial degradation.

pK_a Determination of the Ligands. Total ligand (= L) was 1 mM for L = Me₃tach¹⁹ (0.1 M KCl), 1 mM for L = MeL^a (0.1 M KCl, 0.1 M KNO₃) and 2 mM for L = MeL^a (1.0 M KCl, 1.0 M KNO₃).

Metal Complex Formation. Complete equilibration was always checked by performing back-titrations, and the data was only considered, if no hysteresis was observed. The total amount of L and M used in the various titration experiments is given in the Supporting Information.

Calculations of Equilibrium Constants. Equilibrium constants were calculated as concentration quotients (pH = -log [H⁺]) using the computer programs HYPERQUAD and SPECFIT.^{26,27} The total concentrations of the metals, of L^a and of MeL^a were generally used as fixed values, however, the amount of total Me₃tach and of total H sometimes required some minor adjustments. The values of pK_w (13.78 or 13.77 for I = 0.1 M or 1.0 M) were taken from the literature and were not refined.²⁸ The protonation constants¹⁰ were evaluated separately, and were kept fixed while refining formation constants of the metal-containing species. For the evaluation of the Vis data, the spectra of the free Ni²⁺ and Cu²⁺ were also recorded separately and were imported as fixed data sets. The free MeL^a and its protonation products were treated as non absorbing species. For the evaluation of the potentiometric data, several titration curves were recorded in each case. They were combined to one single data file for a final evaluation. A list of the number of curves, the total ligand : total metal ratio, number of data points, and the pH-range used in each evaluation is given in the Supporting Information.

Single Crystal X-ray Diffraction Studies. Details of data collection and structure solution are listed in Tables 1 and 2. Graphite monochromated Mo-K_α radiation (λ = 0.71073 Å) was used throughout. The structures were solved by direct methods (SHELXS-97) and refined by full-matrix, least-squares calculations on F² (SHELXL-97).²⁹ Anisotropic displacement parameters were refined for all non-hydrogen atoms except for the

(25) Steinhauser, S.; Heinz, U.; Bartholomä, M.; Weyhermüller, T.; Nick, H.; Hegetschweiler, K. *Eur. J. Inorg. Chem.* **2004**, 4177.

(26) Gans, P.; Sabatini, A.; Vacca, A. *Talanta* **1996**, *43*, 1739.

(27) (a) Binstead, R. A.; Jung, B.; Zuberbühler, A. D. *Specfit/32*, Version 3.0; Spectrum Software Associates: Marlborough, MA, 2000. (b) Gampp, H.; Maeder, M.; Meyer, C. J.; Zuberbühler, A. D. *Talanta* **1985**, *32*, 95.

(28) Smith, R. M.; Martell, A. E.; Motekaitis, R. J. *Critically Selected Stability Constants of Metal Complexes*, NIST Standard Reference Database 46; Version 8.0; Gaithersburg, MD, 2004.

(29) Sheldrick, G. M. *Acta Crystallogr., Sect. A* **2008**, *64*, 112.

(23) Bartholomä, M.; Gisbrecht, S.; Stucky, S.; Neis, C.; Morgenstern, B.; Hegetschweiler, K. *Chem.—Eur. J.* **2010**, *16*, 3326.

(24) Ries, A.; Hegetschweiler, K. *NMR-Tit, Program for the Simulation of pH Dependent Shifts in NMR Spectra*, Version 2.0; Saarbrücken, 1999.

Table 1. Crystallographic Data for the Protonated Ligands 2,4,6-H₂Me₃tach(*para*-O₃S-C₆H₄-CH₃)₂, (H₃MeL^a)(BiCl₆)·2H₂O, and (H₃MeL^a)(ClO₄)Cl₂

	H ₂ Me ₃ tach(tos) ₂	H ₃ MeL ^a BiCl ₆	H ₃ MeL ^a ClO ₄ Cl ₂
chem formula	C ₂₃ H ₃₇ N ₃ O ₆ S ₂	C ₆ H ₂₂ BiCl ₆ N ₃ O ₂	C ₆ H ₁₈ Cl ₃ N ₃ O ₄
fw	515.68	589.95	302.58
space group	<i>P</i> $\bar{1}$ (No. 2)	<i>P</i> $\bar{1}$ (No. 2)	<i>Pbca</i> (No. 61)
cryst. system	triclinic	triclinic	orthorhombic
<i>a</i> , Å	9.280(2)	7.5641(3)	10.0794(7)
<i>b</i> , Å	9.951(2)	8.4708(4)	12.1531(8)
<i>c</i> , Å	15.008(3)	14.5577(6)	19.5908(11)
α , deg	102.45(3)	96.546(2)	90.00
β , deg	104.09(3)	104.187(2)	90.00
γ , deg	91.03(3)	103.400(2)	90.00
<i>V</i> , Å ³	1309.0(5)	865.15(6)	2399.8(3)
cryst. dimensions, mm	0.50 × 0.30 × 0.20	0.34 × 0.33 × 0.18	0.20 × 0.15 × 0.10
ρ_{calcd} , g cm ⁻³	1.308	2.265	1.675
μ , mm ⁻¹	0.245	11.114	0.768
<i>Z</i>	2	2	8
diffractometer	STOE IPDS	Bruker X8 Apex	Bruker X8 Apex
<i>T</i> , K	200(2)	100(2)	100(2)
max., min transmission	<i>a</i>	0.2396, 0.1162	0.9272, 0.8616
θ_{max}	24.01	47.90	26.00
data, param.	3783, 348	16068, 178	2358, 173
$R_1 [I > 2\sigma(I)]^b$	0.0452	0.0236	0.0277
wR_2 (all data) ^c	0.1307	0.0580	0.0764
max/min res. e-density, e Å ⁻³	0.494/−0.414	1.988/−3.985 ^d	0.474/−0.405

^a An absorption correction was not performed. ^b $R_1 = \sum ||F_o| - |F_c|| / \sum |F_o|$. ^c $wR_2 = [\sum w(F_o^2 - F_c^2)^2 / \sum wF_o^4]^{1/2}$. ^d Min. and max. of residual electron density were located in a distance of 0.64 Å and 0.53 Å from the Bi atom, respectively.

Table 2. Crystallographic Data for the Co^{III}-Complexes **1**(ClO₄)₃·H₂O and **2**Br₂·H₂O, the Fe^{III}-Complex **3**(ClO₄)₃·0.8MeCN·0.2MeOH, the Dinuclear Cd^{II} Complex **4**, and the Cu^{II} Complexes **5**Br₂·0.5MeOH and **6**·H₂O

	1 ³⁺	2 ³⁺	3 ³⁺	4	5 ²⁺	6
chem formula	C ₁₂ H ₃₂ Cl ₃ - CoN ₆ O ₁₃	C ₁₂ H ₃₂ Br ₃ - CoN ₆ O	C _{13.8} H _{33.2} Cl ₃ - FeN _{6.8} O _{12.2}	C ₁₂ H ₃₀ Cd ₂ - Cl ₄ N ₆	C _{12.5} H ₃₂ Br ₂ - CuN ₆ O _{0.5}	C ₆ H ₁₈ Br ₃ - CuN ₃ O
fw	633.72	575.10	651.87	625.02	497.80	451.50
space group	<i>P2</i> ₁ / <i>n</i> (No. 14)	<i>Pnma</i> (No. 62)	<i>Pnma</i> (No. 62)	<i>P2</i> ₁ / <i>c</i> (No. 14)	<i>P</i> $\bar{1}$ (No. 2)	<i>P2</i> ₁ / <i>n</i> (No. 14)
cryst. system	monoclinic	orthorhombic	orthorhombic	monoclinic	triclinic	monoclinic
<i>a</i> , Å	10.149(2)	14.707(3)	16.8754(7)	9.3738(19)	8.5750(17)	7.73220(10)
<i>b</i> , Å	16.769(3)	7.2965(15)	8.0046(3)	10.777(2)	10.974(2)	11.6715(2)
<i>c</i> , Å	14.389(3)	18.477(4)	18.9265(8)	10.695(2)	11.730(2)	14.4729(3)
α , deg	90.00	90.00	90.00	90.00	88.27(3)	90.00
β , deg	100.11(3)	90.00	90.00	90.70(3)	76.95(3)	93.7960(10)
γ , deg	90.00	90.00	90.00	90.00	86.59(3)	90.00
<i>V</i> , Å ³	2410.8(8)	1982.8(7)	2556.61(18)	1080.3(4)	1073.3(4)	1303.26(4)
cryst. dimensions, mm	0.30 × 0.20 × 0.15	0.30 × 0.20 × 0.10	0.30 × 0.15 × 0.10	0.30 × 0.20 × 0.10	0.20 × 0.15 × 0.10	0.30 × 0.20 × 0.05
ρ_{calcd} , g cm ⁻³	1.746	1.927	1.694	1.921	1.540	2.301
μ , cm ⁻¹	1.119	6.923	0.975	2.471	4.748	10.850
<i>Z</i>	4	4	4	2	2	4
diffractometer	STOE Stadi 4	STOE IPDS	Bruker X8 Apex	STOE IPDS	STOE IPDS	Bruker X8 Apex
<i>T</i> , K	298(2)	200(2)	100(2)	200(2)	200(2)	100(2)
max., min transmission	<i>a</i>	0.5444, 0.2305	0.9088, 0.7585	0.7902, 0.5244	0.6482, 0.4502	0.6130, 0.1392
θ_{max}	25.00	26.00	25.99	25.99	28.07	37.22
data, param.	4240, 378	2102, 141	2669, 213	2098, 125	5084, 215	6517, 153
$R_1 [I > 2\sigma(I)]^b$	0.0459	0.0327	0.0500 ^d	0.0244	0.0629	0.0344
wR_2 (all data) ^c	0.1197	0.0786	0.1538 ^d	0.0622	0.1720	0.0653
max/min res. e-density, e Å ⁻³	1.052/−0.661	1.570/−0.927	0.841/−0.645 ^d	1.011/−0.457	1.308/−1.110	1.030/−0.871

^a An absorption correction was not performed. ^b $R_1 = \sum ||F_o| - |F_c|| / \sum |F_o|$. ^c $wR_2 = \sum w(F_o^2 - F_c^2)^2 / \sum wF_o^4]^{1/2}$. ^d After treatment of the disordered solvent using the Program Squeeze of the PLATON package,³⁰ see text in the Experimental Section.

disordered MeOH molecule in **5**Br₂·0.5MeOH (vide infra). Puckering parameters were calculated using the computer program PLATON.³⁰

Disorder. H₂Me₃tach(tos)₂: The oxygen atom O23 of one of the two sulfonate groups was found to be distributed over two sites (A and B) with occupancies of 45 and 55%. One ClO₄[−] anion (Cl3, O9–O12) of **1**(ClO₄)₃·H₂O was refined as a major (A, 60%) and a minor (B, 40%) component. All three

perchlorate anions of **3**(ClO₄)₃·0.8MeCN·0.2MeOH were located on a mirror plane, but only one of them (Cl1, O1–O3) was well ordered. The second anion was distributed over three sites Cl2A (60%), Cl2B (20%), and Cl2C (20%); the third anion was refined with a fully occupied Cl3 and O11 and with each two half occupied positions for O9 and O10. An additional MeCN molecule was located. However, the displacement ellipsoids of its C and N atoms deviated significantly from an ideal shape. Moreover, inspection of a difference Fourier map indicated some remaining peaks in proximity to this solvent molecule. At this stage, the agreement factors were $R_1 = 0.0606$ and $wR_2 = 0.1873$. The result was interpreted in terms of a superposition of

(30) Spek, A. L. *PLATON, A Multipurpose Crystallographic Tool*; Utrecht University: Utrecht, The Netherlands, 2005; see also: Spek, A. L. *J. Appl. Crystallogr.* **2003**, *36*, 7.

a MeCN and a MeOH molecule, sharing the same position at random. Attempts to resolve the disorder were, however, not successful. The program SQUEEZE of the PLATON package³⁰ was therefore applied to the data set and an amount of 20 electrons per cation 3^{3+} was subtracted from the electron density, resulting in $R_1 = 0.0500$ and $wR_2 = 0.1538$. The amount of 20 e^- is in agreement with a formulation $3(\text{ClO}_4)_3 \cdot x\text{MeCN} \cdot (1-x)\text{MeOH}$. According to the elemental analysis $x \approx 0.8$. One of the counterions of $5\text{Br}_2 \cdot 0.5\text{MeOH}$ (Br2) was distributed over two sites in a 70% to 30% ratio. Moreover, the MeOH molecule was only half occupied, and its methyl group was distributed equally over two sites, having thus occupancy factors of 0.25.

Treatment of Hydrogen Atoms. Calculated positions (riding model) were generally used for H(-C) atoms. The H(-N) positions of $(\text{H}_3\text{MeL}^a)(\text{BiCl}_6) \cdot 2\text{H}_2\text{O}$, $3(\text{ClO}_4)_3 \cdot 0.8\text{MeCN} \cdot 0.2\text{MeOH}$ and $5\text{Br}_2 \cdot 0.5\text{MeOH}$ were also calculated. All other H(-N) positions were refined using isotropic displacement parameters. In $(\text{H}_3\text{MeL}^a)(\text{ClO}_4)_2$, a restraint was used to fix the N3–H3NA distance to a value of 0.88 Å. H(-O) atoms could not be located and were not considered in the refinement except for $(\text{H}_3\text{MeL}^a)(\text{BiCl}_6) \cdot 2\text{H}_2\text{O}$, $1(\text{ClO}_4)_3 \cdot \text{H}_2\text{O}$, and $6 \cdot \text{H}_2\text{O}$, where the H(-O) positions were refined isotropically. For $1(\text{ClO}_4)_3 \cdot \text{H}_2\text{O}$ restraints were used to fix the two O–H distances to a value of 0.82 Å. For $6 \cdot \text{H}_2\text{O}$ and $(\text{H}_3\text{MeL}^a)(\text{BiCl}_6) \cdot 2\text{H}_2\text{O}$, the O–H distances were restrained to 0.84 Å with U_{iso} of the H atoms being set to $1.5 \times U_{\text{eq}}$ of the pivotal O atom.

Molecular Mechanics Calculations. These were carried out as described previously²³ using the program HYPERCHEM³¹ for visualization and the program MOME97³² with an extended force field³³ for structure optimization and energy minimization. It has been shown that the MOME97 force field reproduces the structures of low-spin- Co^{III} -amine complexes reliably, and calculates meaningful differences for the strain energy of diastereomeric complexes.^{34,35} Therefore metal complexes were generally modeled with Co^{III} . In a first step, geometry optimization was performed with the full-matrix Newton–Raphson algorithm. To avoid location of false (local) minima, a search for further low-energy conformers was performed using the *Random Kick* option, and in some cases structures of considerably lower energy were indeed found. They were then energy minimized once more. All energy minimization calculations converged (<0.001 Å) without problems, and the calculated structures generally exhibited meaningful bond distances and angles. Several different conformers were considered for the free ligands, and the data presented in this paper always correspond to the least strained. Of the possible diastereomeric L^a - and MeL^a -*bis*-complexes, the *cis*-isomers revealed to be the less strained. For L^b and MeL^b the reverse result was observed, that is, the *trans*-isomers were slightly more stable. The chelate rings in $[\text{Co}(\text{tacn})_2]^{3+}$ can have either a λ or δ conformation. It is generally accepted that within one coordinated tacn entity, the lowest energy corresponds to three chelating rings of the same type.³⁶ Regarding the two ligands in the *bis*-complex, a chiral

Table 3. $\text{p}K_{\text{ai}}$ ($= -\log K_{\text{ai}}$) Values of Triply Protonated Triamines H_3L^{3+} at 25 °C with Estimated Uncertainties (3σ) in Parentheses

(a) Comparison of Some Relevant Triamines at an Ionic Strength of $I = 0.1$ M						
amine (L)	tach	2,4,6- Me_3tach	1,3,5- Me_3tach	L^a	tacn	
$\text{p}K_{\text{a1}}$	7.17 ^b	5.15 ^c	5.18(2) ^d	5.0 ^e	3.20 ^f	$< 2^b$
$\text{p}K_{\text{a2}}$	8.66 ^b	6.73 ^c	7.35(1) ^d	8.5 ^e	6.47 ^f	6.81 ^b
$\text{p}K_{\text{a3}}$	10.16 ^b	7.83 ^c	11.24(1) ^d	$> 12^e$	9.24 ^f	10.44 ^b

(b) Values for $(\text{H}_3\text{MeL}^a)^{3+}$ in Different Media As Indicated						
	0.1 M KNO_3	0.1 M KCl	1.0 M KCl	1.0 M KNO_3	D_2O	
$\text{p}K_{\text{a1}}$	1.93(1) ^d	1.93(1) ^d	2.30(1) ^d	2.36(1) ^d	1.91 ^{d,g}	2.10 ^h
$\text{p}K_{\text{a2}}$	6.32(1) ^d	6.33(1) ^d	6.66(1) ^d	6.65(1) ^d	6.70 ^{d,g}	6.37 ^h
$\text{p}K_{\text{a3}}$	9.18(1) ^d	9.19(1) ^d	9.39(1) ^d	9.38(1) ^d	9.54 ^{d,g}	9.26 ^h

^a $K_{\text{ai}} = [\text{LH}_3-i] \times [\text{H}] \times [\text{LH}_{4-i}]^{-1}$. ^b From reference 28. ^c From reference 13. ^d This work. ^e From reference 14a. ^f From reference 10. ^g Evaluation of the NMR titration (no inert electrolyte, ambient temperature). ^h From reference 8, ionic strength not specified.

$(\lambda,\lambda,\lambda)(\lambda,\lambda,\lambda)$ [or $(\delta,\delta,\delta)(\delta,\delta,\delta)$] conformer with D_3 symmetry or a $(\lambda,\lambda,\lambda)(\delta,\delta,\delta)$ conformer with S_6 symmetry must be considered. Inspection of the Cambridge Structural Database revealed examples for both types in corresponding crystal structures (Supporting Information, Table S1). According to our calculations, the chiral D_3 conformer is slightly less strained, and the data used in our study refer thus to this particular structure.

Results

Characterization of Me_3tach .¹⁹ It has already been shown by Parker et al. that Me_3tach and the fully protonated $\text{H}_3\text{Me}_3\text{tach}^{3+}$ adopt reverse chair conformations with the three nitrogen atoms in either axial or equatorial positions.¹³ Parker also studied the stepwise protonation of Me_3tach , and found a remarkably low basicity for this triamine (Table 3a). A conformation with equatorial nitrogen donors was proposed for the doubly protonated species, and the low basicity was attributed to a particularly favorable intramolecular hydrogen bonding between the axial amino groups of the neutral triamine, that is destroyed upon protonation. This explanation appears, however, not to be fully conclusive, since it is generally assumed that hydrogen bonds between free amino groups are only weak.^{16,37} The low basicity of 2,4,6- Me_3tach also contradicts a report of Menger et al. who found a high basicity for the isomeric 1,3,5- Me_3tach .^{14a} We therefore decided to repeat the $\text{p}K_{\text{a}}$ determination of 2,4,6- $\text{H}_3\text{Me}_3\text{tach}^{3+}$ and found indeed a significantly higher first protonation constant (Table 3a) than the one reported by Parker et al.

An NMR titration proved helpful to identify the individual conformations of the variably protonated species (Figure 1). The behavior displayed in Figure 1 becomes clear, if one considers that proton transfer reactions are generally fast within the NMR time scale, whereas conversion of the two chair conformations of these rigid molecules is slow. As a consequence, averaged signals are observed for species with the same conformation but a different degree of protonation, whereas distinct signals are generally observed for species with different conformations.

(37) Reiss, G. J.; Zimmer, A.; Hegetschweiler, K. *Acta Crystallogr., Sect. C* **2000**, *56*, 284.

(31) *HyperChem, Release 7.51 for Windows*; Hypercube Inc.: Gainesville, FL, 2002.

(32) (a) Comba, P.; Hambley, T. W.; Lauer, G.; Okon, N. *MOME97, a molecular modeling package for inorganic compounds*; University of Heidelberg: Heidelberg, Germany, 1997. (b) Bol, J. E.; Buning, C.; Comba, P.; Reedijk, J.; Ströhle, M. *J. Comput. Chem.* **1998**, *19*, 512. (c) Comba, P.; Hambley, T. W. *Molecular modeling of inorganic compounds*; VCH: Weinheim, Germany, 1995.

(33) Kuppert, D.; Comba, P.; Hegetschweiler, K. *Eur. J. Inorg. Chem.* **2006**, 2792.

(34) Bygott, A. M. T.; Sargeson, A. M. *Inorg. Chem.* **1998**, *37*, 4795.

(35) Comba, P.; Maeder, M.; Zipper, L. *Helv. Chim. Acta* **1989**, *72*, 1029.

(36) (a) Boeyens, J. C. A.; Dobson, S. M.; Hancock, R. D. *Inorg. Chem.* **1985**, *24*, 3073. (b) Boeyens, J. C. A.; Forbes, A. G. S.; Hancock, R. D.; Wiegardt, K. *Inorg. Chem.* **1985**, *24*, 2926. (c) Pletnev, I. V. *Can. J. Chem.* **1994**, *72*, 1404. (d) Gao, Y.-D.; Lipkowitz, K. B.; Schultz, F. A. *J. Am. Chem. Soc.* **1995**, *117*, 11932. (e) Golding, S. W.; Hambley, T. W.; Lawrance, G. A.; Luther, S. M.; Maeder, M.; Turner, P. *J. Chem. Soc., Dalton Trans.* **1999**, 1975.

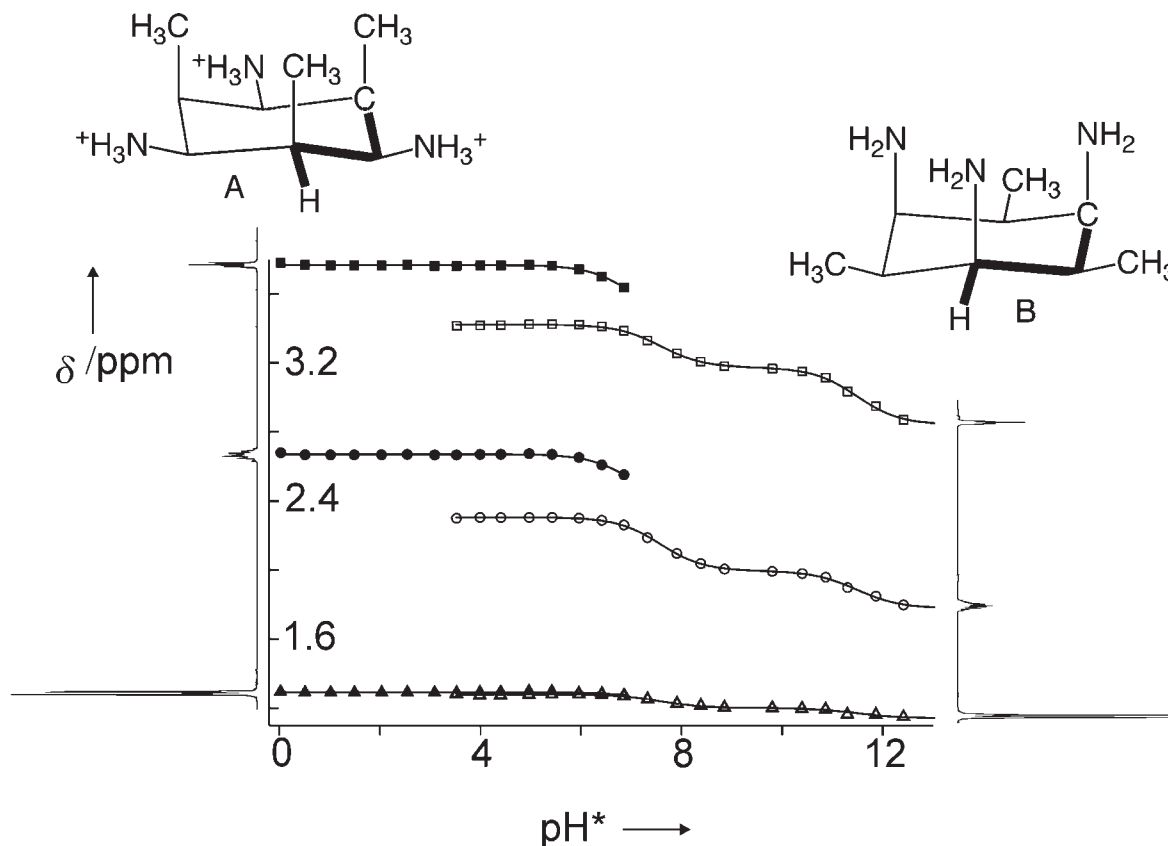


Figure 1. pH* dependence¹⁷ of the ¹H NMR resonances of H_xMe₃tach^{x+} (0 ≤ x ≤ 3).¹⁹ Closed and open squares, circles, and triangles refer to H(-C-N)-, H(-C-CH₃)-, and CH₃-resonances of the conformers having either equatorial nitrogen atoms (A) or equatorial methyl groups (B), respectively. The lines were calculated (minimization of $\sum(\delta_{\text{obs}} - \delta_{\text{calcd}})^2$). Bold bonds in the two formulas represent the three-bond long-range C-H coupling pathway which was used to identify the two conformers.

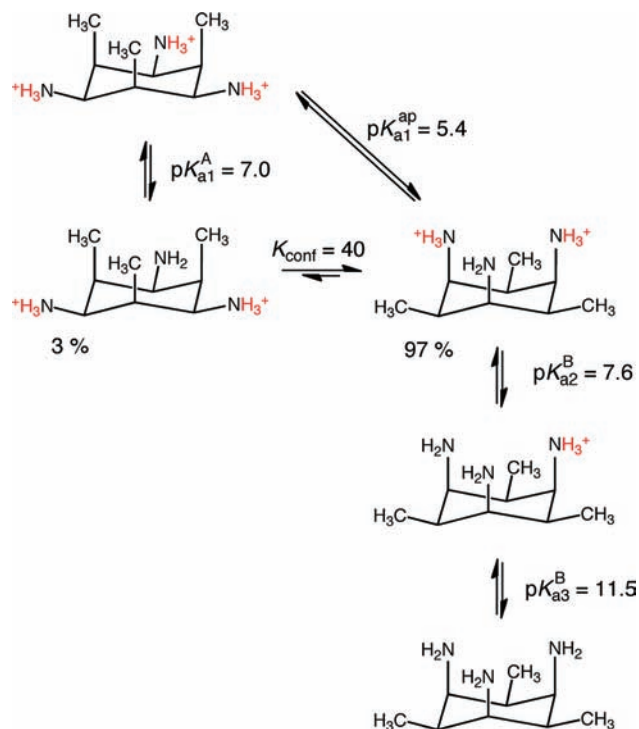
In Figure 1, the two possible chair forms with equatorial or axial nitrogen donors are denoted as A and B. They were unambiguously identified by a series of 2D C-H long-range experiments. At pH* < 3, the triply protonated (H₃Me₃tach^A)³⁺ is the sole species.^{17,19} The chemical shifts of its signals become pH-dependent at pH* ≥ 6, indicating thus a subsequent deprotonation to (H₂Me₃tach^A)²⁺. This pH dependence was used to calculate a corresponding pK_{a1}^A of 7.0. The value compares well with 7.2 listed for pK_{a1} of the parent H₃tach³⁺ (Table 3a), that also has the amino groups exclusively in equatorial positions. An additional component with conformation B appeared above pH 3.5. It is deprotonated in two steps as shown by the characteristic sigmoid shape in the range 6 ≤ pH* ≤ 9 and 10 ≤ pH* ≤ 13. Consequently, these species were formulated as (H₂Me₃tach^B)²⁺, (HMe₃tach^B)⁺ and Me₃tach^B with pK_{a2}^B = 7.6 and pK_{a3}^B = 11.5. It should be noted that all these pK_a values refer to one specific conformer and must be regarded as so-called “micro-constants” (Scheme 1). In the range 3.5 ≤ pH* ≤ 5.5 the two predominant species are thus (H₃Me₃tach^A)³⁺ and (H₂Me₃tach^B)²⁺, which are in equilibrium, and the apparent pK_{a1}^{ap} = 5.4 corresponds to the reaction (H₃Me₃tach^A)³⁺ = (H₂Me₃tach^B)²⁺ + H⁺. It can be calculated directly from the integrals of the NMR-signals using the Henderson–Hasselbalch equation. Since (H₃Me₃tach^A)³⁺ and (H₂Me₃tach^B)²⁺ are the only significant species in this range, pK_{a1}^{ap} is in close agreement with the true macroscopic pK_{a1} of H₃Me₃tach³⁺; the agreement with

pK_{a1} = 5.2 obtained from the potentiometric study (Table 3a) is indeed good. pK_{a1}^{ap} and pK_{a1}^A can be used to calculate the equilibrium constant K_{conf} for the chair conversion of H₂Me₃tach²⁺ which is K_{conf} = 40, in favor for conformer B. This means that the doubly protonated H₂Me₃tach²⁺ is present, in contrast to Parker’s prediction, to about 97% in the form with axial nitrogen atoms. The low amount of form A of the doubly protonated species is the reason that the trace of this conformer is lost in the NMR-titration curve above pH* > 7.5.

Weak hydrogen bonding between the neutral amino groups but strong hydrogen bonding between an amino and an ammonium group is reflected in the observation that 2,4,6-Me₃tach and 1,3,5-Me₃tach are both stronger bases than the parent tach. Moreover, ΔpK_a = pK_{a3} - pK_{a2} of Me₃tach¹⁹ is 3.9, and this difference is significantly higher than for tach (ΔpK_a = 1.5, see Table 3a),²⁸ confirming strong mutual electrostatic interactions between two *axial* ammonium groups in H₂Me₃tach²⁺.³⁸ An axial orientation of the nitrogen atoms in the doubly protonated form was finally confirmed by a crystal structure analysis of (H₂Me₃tach)(*para*-O₃S-C₆H₄-CH₃)₂. The structure (Figure 2) also showed the expected strong intramolecular hydrogen bonding between an amino and an ammonium group, and the significant electrostatic repulsion between the two positive charges in terms of a characteristic distortion from an ideal chair form.

(38) Hegetschweiler, K.; Erni, I.; Schneider, W.; Schmalle, H. *Helv. Chim. Acta* **1990**, *73*, 97.

Scheme 1. Protonation and Conformational Rearrangement of $H_xMe_3tach^{x+}$ ($0 \leq x \leq 3$)¹⁹ As Deduced from pH*-Dependent ¹H NMR Measurements (Figure 1)



Obviously, addition of the first proton results in a particularly favorable intramolecular hydrogen bonding pattern (“chelated proton”).¹⁶ With regard to preorientation of the donor set, one can thus state that the three amino groups of 2,4,6- Me_3tach (and probably also of 1,3,5- Me_3tach) are, in contrast to the parent $tach$, almost ideally arranged for metal binding.

Characterization of MeL^a . The situation for the diazepane based L^a and MeL^a is more complex. It is well-known that cycloheptane is conformationally flexible. A series of chair- (C) and twist-chair (TC) conformations with rather low barriers between them (pseudo rotation), constitute the low energy forms, and it has been shown that the TC conformation is most favorable.⁴⁰ In contrast to the rigid cyclohexane chair (D_{3d}), the symmetry of TC-cycloheptane is low (C_2) having one unique isoclinal and three distinct (pseudo)-axial and (pseudo)-equatorial positions (Figure 3). For methylcycloheptane, lowest energy is observed for the three TC conformers with the methyl group in one of the equatorial positions; for 1,1-dimethylcycloheptane the TC conformation of lowest energy has the two methyl groups in the isoclinal positions.⁴¹ Derivatives with one or two hetero atoms within the cycloheptane ring have been studied less intensively.^{42,43} It is believed, at least for neutral species, that some of the

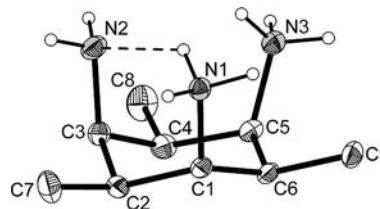


Figure 2. Molecular structure of the $H_2Me_3tach^{2+}$ cation showing a chair conformation of the cyclohexane ring. The hydrogen bonding scheme is in agreement with the different $N \cdots N$ distances: $N1 \cdots N2$ 2.854(3) Å, $N1 \cdots N3$ 3.475(3) Å, $N2 \cdots N3$ 3.134(4) Å. Angles: $N1-H11 \cdots N2$ 131(2)°, $N3-H31 \cdots N2$ 125(2)°. Owing to the asymmetric hydrogen bonding and the repulsion between the two positive ammonium groups, the cyclohexane chair shows some distortion toward a half chair conformation (puckering parameters: $Q = 0.533$ Å, $\theta = 169^\circ$, $\phi = 276^\circ$).³⁹ The displacement ellipsoids are drawn at the 30% probability level; H(-N) hydrogen atoms are shown as spheres of arbitrary size; H(-C) hydrogen atoms are omitted for clarity.

axial substitutions are less disfavored. For the triamines L^a and MeL^a , protonation must again be considered, and it is obvious that the additional electrostatic repulsion between the positive charges will influence the conformational equilibrium.

In the crystal structure of $(H_3L^a)Cl_3 \cdot H_2O$, described in our previous contribution,¹⁰ $(H_3L^a)^{3+}$ adopted a TC conformation with the two ring nitrogen atoms in position 1 and 4' (Figure 3). The primary ammonium group, which is attached to C3, has an equatorial orientation. The corresponding $(H_3MeL^a)^{3+}$ cation has been crystallized as $(H_3MeL^a)(BiCl_6) \cdot 2H_2O$ and $(H_3MeL^a)(ClO_4)_2 \cdot Cl_2$. In both salts, the seven membered ring adopts again a TC conformation. However, the two substituents are either located in position 1 (both isoclinal) or 4 (axial CH_3 , equatorial NH_3^+), respectively. The adoption of different TC conformations in the two salts is consistent with the minor difference in energy for such conformers, and is obviously due to specific packing interactions (Supporting Information, Figure S1 and Table S2).⁴⁴

The ¹H NMR titration and pK_a determination (Table 3a) of $(H_3L^a)^{3+}$ have already been reported. The pK_a values of the methylated $(H_3MeL^a)^{3+}$ have been determined by Peralta et al.,⁸ however, without specifying an ionic strength. We repeated the determination of these values and obtained an acceptable agreement (Table 3b). Obviously the basicity of L^a and MeL^a is quite similar. The observation of five signals in the ¹H- and four signals in the ¹³C NMR spectrum of MeL^a is in agreement with a rapid equilibrium between the different conformers and C_2 or C_s symmetry for the averaged structure. The signals exhibited a characteristic pH dependence (Supporting Information, Figure S2). The ¹H NMR titration curve

(44) In $(H_3MeL^a)(ClO_4)_2$ and $(H_3MeL^a)(BiCl_6) \cdot 2H_2O$, the $(H_3MeL^a)^{3+}$ cations are involved in an extensive network of hydrogen bonding (Supporting Information, Table S2). Both structures can be regarded as distortions of a faced centered cubic (fcc) packing of the cations with the ClO_4^- or $[BiCl_6]^{3-}$ anions in the octahedral and the Cl^- anions or H_2O molecules in the tetrahedral holes (Supporting Information, Figure S1). The packing of the latter is significantly compressed along one of the pseudo- C_3 -axes. The structure represents thus an intermediate between the fcc NaCl and the simple cubic CsCl structure: Each $(H_3MeL^a)^{3+}$ has six neighboring $[BiCl_6]^{3-}$ anions arranged in a distorted octahedral fashion with cation–anion distances ranging from 5.5–7.1 Å (average: 6.1 Å, measured from the center of gravity). Two additional anions with cation–anion distances of 8.8 and 9.3 Å are placed at some longer distances. These distances are, however, shorter than expected for a true fcc structure ($\sqrt{3} \times 6.1$ Å = 10.6 Å).

(39) Cremer, D.; Pople, J. A. *J. Am. Chem. Soc.* **1975**, *97*, 1354.

(40) Eliel, E. L.; Allinger, N. L.; Angyal, S. J.; Morrison, G. A. *Conformational Analysis*; Interscience Publishers, John Wiley: New York, 1965.

(41) Hendrickson, J. B. *J. Am. Chem. Soc.* **1962**, *84*, 3355.

(42) (a) Espinosa, A.; Gallo, M. A.; Entrena, A.; Gomez, J. A. *J. Mol. Struct.* **1994**, *326*, 249. (b) Entrena, A.; Campos, J.; Gomez, J. A.; Gallo, M. A.; Espinosa, A. *J. Org. Chem.* **1997**, *62*, 337. (c) Entrena, A.; Campos, J. M.; Gallo, M. A.; Espinosa, A. *ARKIVOC* **2005**, 88.

(43) Sengar, R. S.; Geib, S. J.; Nigam, A.; Wiener, E. C. *Acta Crystallogr., Sect. C* **2010**, *66*, o174.

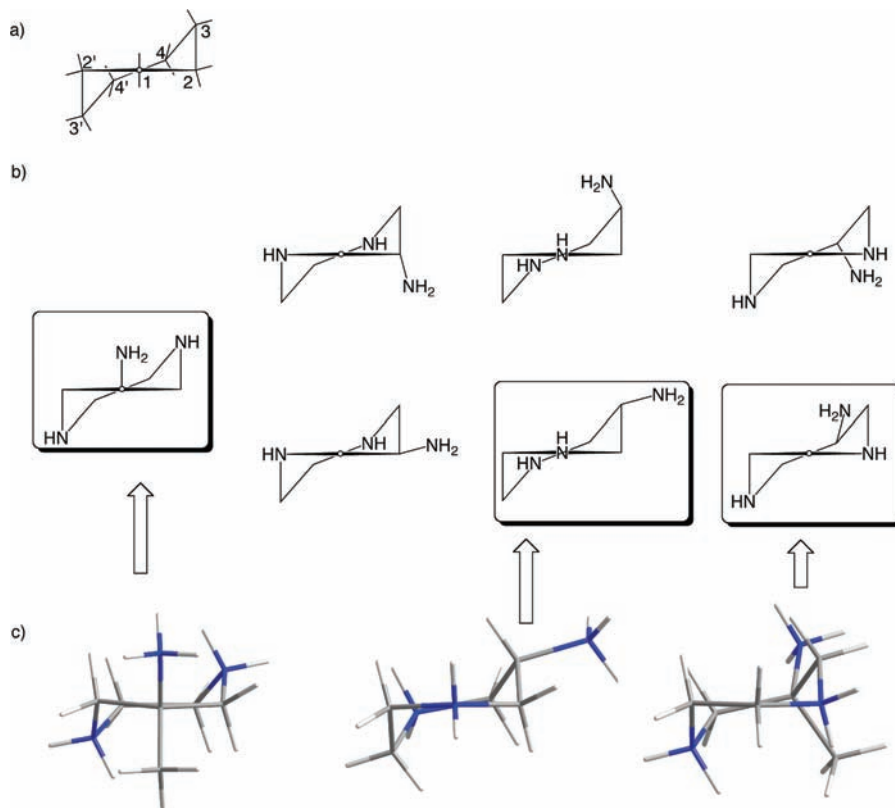


Figure 3. Possible twist chair (TC) conformations of the 6-amino-1,4-diazepane frame. (a) Numbering scheme for the C_2 -symmetric seven membered ring; 1 refers to the unique isoclinal position, placed on the 2-fold rotational axis. (b) The possible conformers with the primary amino group in an axial (upper row) or an equatorial (lower row) position. (c) Molecular structure of $(H_3MeL^a)^{3+}$ and $(H_3L^a)^{3+}$ as obtained from crystal structure analysis of $(H_3MeL^a)BiCl_6 \cdot 2H_2O$ (this work), $(H_3L^a)Cl_3 \cdot H_2O^{10}$ and $(H_3MeL^a)(ClO_4)Cl_2$ (this work). A stick model with white (H), gray (C), and blue (N) color is used for the representation of the structures.

could be used to estimate the equilibrium between the different tautomers of the partially protonated species.⁴⁵ Similar to L^a , the first protonation of MeL^a is not specific. In contrast, one single tautomer with protonation of the primary amino group is observed for the doubly protonated $(H_2MeL^a)^{2+}$.⁴⁶ Molecular modeling calculations predict very similar strain energies for several different TC conformations ($\Delta E \leq 1 \text{ kJ mol}^{-1}$).

Solid State Structures of Metal Complexes. A mixture of the *cis*- and *trans*-isomer of $[Co^{III}(MeL^a)_2]^{3+}$ (1^{3+} and 2^{3+}) were prepared by an aerial oxidation of an $MeL^a/CoCl_2$ solution. The two diastereomers could be separated on a Sephadex column and were isolated in amounts of 19% and 40%. On the basis of the different symmetry (C_2 and C_{2h}) they could be identified unambiguously by 1H and ^{13}C NMR-spectroscopy. Both complexes have a typical $Co^{III}N_6$ chromophore. As expected, the non-centrosymmetric *cis*-isomer 1^{3+} displayed bands of higher intensity in the UV/vis spectrum (Supporting Information, Table S3). The structural assignment was also confirmed by a crystal structure analysis of $1(ClO_4)_3 \cdot H_2O$

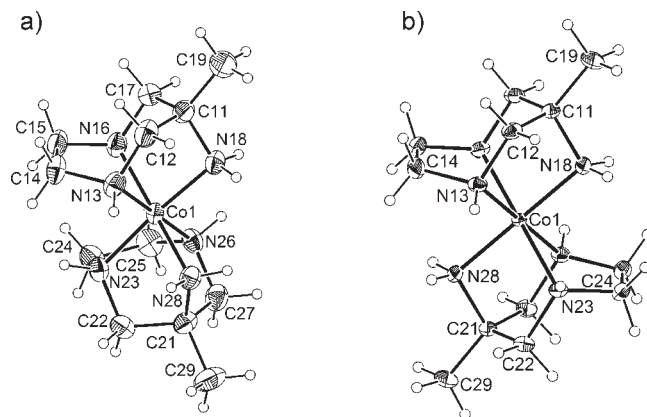


Figure 4. Molecular structure of (a) *cis*- $[Co(MeL^a)_2]^{3+}$ (1^{3+}), and (b) *trans*- $[Co(MeL^a)_2]^{3+}$ (2^{3+}). The displacement ellipsoids are drawn at the 50% probability level; hydrogen atoms are shown as spheres of arbitrary size.

and $2Br_3 \cdot H_2O$ (Figure 4). Orange-red crystals containing the *trans*- $[Fe(MeL^a)_2]^{3+}$ (3^{3+}) cation (Supporting Information, Figure S3) were grown in a MeOH/MeCN/EtOAc medium. The crystal structure of $3(ClO_4)_3 \cdot 0.8MeCN \cdot 0.2MeOH$ exhibited some disorder for the ClO_4^- counterions and in particular for the solvent molecules (see the Experimental Section). The molecular structure of the two *trans*-complexes 2^{3+} and 3^{3+} are virtually identical. Although the two metal centers are located on positions with crystallographically imposed m site symmetry, the deviation from a centrosymmetric structure (C_{2h}) is not

(45) Sudmeier, J. L.; Reilly, C. N. *Anal. Chem.* **1964**, *36*, 1698.

(46) The characteristic pH-dependence of the diaminoethylene H(-C) resonances was used to estimate the ratio of tautomers for $(HMeL^a)^+$ and $(H_2MeL^a)^{2+}$ (calculations for the CH_2 groups in β -position to NH_2 exhibited very similar shifts for the different tautomers and are thus not suited for such an analysis). The deshielding constants $C(\alpha) = 0.633 \text{ ppm}$, $C(\alpha) = 9C(\gamma)$ and $C(\beta) = 5C(\gamma)$, which were derived from the fully protonated $(H_3MeL^a)^{3+}$ and the deprotonated MeL^a ,^{6,7,45} revealed amounts of 42% and 95% for a protonation of the primary amino group in $(HMeL^a)^+$ and in $(H_2MeL^a)^{2+}$, respectively.

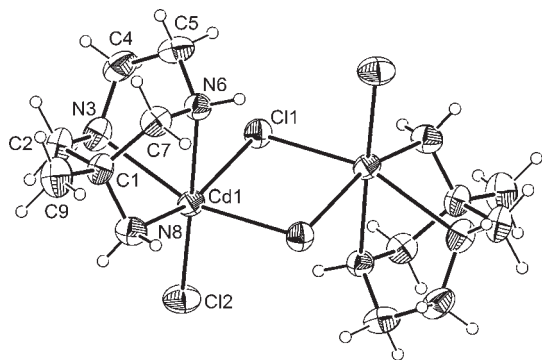


Figure 5. Molecular structure of $[(\text{MeL}^a)\text{ClCd}(\mu_2\text{-Cl})_2\text{-CdCl}(\text{MeL}^a)]$ (**4**). The thermal ellipsoids are drawn at the 50% level; hydrogen atoms are shown with arbitrary size.

significant. Both metal cations were found to be in the low spin state. The presence of one single unpaired electron in the Fe^{III} complex **3**³⁺ was confirmed by magnetic susceptibility measurements (Evans method).⁴⁷ All three complexes **1**³⁺–**3**³⁺ form generally longer M–N bonds to the secondary (endocyclic) amino groups, and the M–N bond distances in the Fe^{III} derivative are, as expected, in general somewhat longer. Because of the crystallographic mirror plane which passes the $\text{N}_{\text{prim}}\text{-M-N}_{\text{prim}}$ moiety of **2**³⁺ and **3**³⁺, the torsion angle of the diamino-ethane group in the *trans*-configured species is exactly 0° and the N–C–C–N fragment receives an unfavorable eclipsed orientation (pure C conformation).

The structure of a *bis*- MeL^a -complex of Ni^{II} and Zn^{II} has already been reported previously by other groups.^{8,48} To get a better understanding how the size of the metal center influences the structure of the ligand framework, single crystals of a Cd^{II} complex (Figure 5) were grown from aqueous solution. The complex was obtained as a chloro-bridged dimer of composition $[(\text{MeL}^a)\text{ClCd}(\mu\text{-Cl})_2\text{CdCl}(\text{MeL}^a)]$ (**4**). A similar dinuclear structure has already been observed for a corresponding dapi complex.⁷ The dihedral N–C–C–N angle in **4** is slightly enlarged compared to metal complexes with smaller metal cations (Table 4).

Single crystals of the Cu^{II} complexes *trans*- $[\text{Cu}(\text{MeL}^a)_2]\text{-Br}_2 \cdot 0.5\text{MeOH}$ (**5Br**₂ · 0.5MeOH, blue) and $[\text{Cu}(\text{HMeL}^a)\text{-Br}_3] \cdot \text{H}_2\text{O}$ (**6** · H₂O, green) were grown from a nonaqueous medium (MeCN/MeOH/EtOAc) and from water at pH ≈ 4, using CuBr_2 and MeL^a as starting materials in a 1:2 or 1:1 molar ratio, respectively. The *bis*-complex **5**²⁺ (Supporting Information, Figure S4) displays a strictly centrosymmetric structure with a characteristic Jahn–Teller distortion (two long bonds formed by secondary, endocyclic amino groups).^{5b,7,14a,23,49}

In **6** · H₂O, the protonated (HMeL^a)⁺ ligand exhibited bidentate coordination with the primary and one of the secondary amino groups bonded to the Cu^{II} center (Figure 6). It is the remaining *endocyclic* amino group which is detached and protonated. In contrast to the molecular

Table 4. Synopsis of Structural Parameters of MeL^a and Their Metal Complexes

	mean M–N _{exo} distance (Å)	mean M–N _{endo} distance (Å)	N _{endo} –C– C–N _{endo} torsional angle (deg)
$(\text{H}_3\text{MeL}^a)(\text{ClO}_4)\text{Cl}_2$			42.1
$(\text{H}_3\text{MeL}^a)(\text{BiCl}_6) \cdot 2\text{H}_2\text{O}$			60.6
<i>cis</i> - $[\text{Co}(\text{MeL}^a)_2]^{3+}$ (1 ³⁺)	1.953	2.007	2.2
<i>trans</i> - $[\text{Co}(\text{MeL}^a)_2]^{3+}$ (2 ³⁺)	1.952	1.993	0.0
<i>trans</i> - $[\text{Fe}(\text{MeL}^a)_2]^{3+}$ (3 ³⁺)	1.979	2.021	0.0
$[\text{Cd}(\text{MeL}^a)\text{Cl}_2]$ (4)	2.334(3)	2.441	4.4
<i>trans</i> - $[\text{Cu}(\text{MeL}^a)_2]^{2+}$ (5 ²⁺)	2.028	2.078, 2.462	2.4
$[\text{CuBr}_3(\text{HMeL}^a)]$ (6)	2.011(2)	2.025(2)	69.7
<i>trans</i> - $[\text{Ni}(\text{MeL}^a)_2]^{2+}$	2.090 ^a	2.125 ^a	0.82 ^a
<i>trans</i> - $[\text{Zn}(\text{MeL}^a)_2]^{2+}$	2.128 ^b	2.202 ^b	0.0 ^b
$[\text{Fe}(\text{MeL}^a)]^{3+}$	2.189 ^c	2.210 ^c	2.6 ^c

^aFrom reference 8. ^bFrom reference 48. ^cIn the tetranuclear $(\mu\text{-O})_2\text{-}(\text{Fe}^{\text{III}}\text{MeL}^a)_4\text{-}\{\mu\text{-H}_2\text{MeL}^a(\text{CO}_2)_2\}_2^{4+}$, see reference 21.

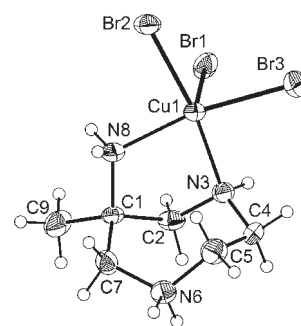


Figure 6. Molecular structure of $[\text{Cu}(\text{HMeL}^a)\text{Br}_3]$ (**6**). The thermal ellipsoids are drawn at the 50% level; hydrogen atoms are shown as spheres of arbitrary size. Puckering parameters: $q_2 = 0.44 \text{ \AA}$, $q_3 = 0.69 \text{ \AA}$, $\phi_2 = 32.4^\circ$, $\phi_3 = 67.8^\circ$.³⁹

structures of **1**–**5**, where the MeL^a entity always adopted a pure chair (C), the ligand framework of **6** · H₂O has a TC conformation (TC5 according to Espinosa's nomenclature)^{42b} with an N_{endo}–C–C–N_{endo} torsion angle of 70°. The coordination geometry of Cu^{II} corresponds basically to a square-pyramidal CuN_2Br_3 -geometry with a minor distortion toward a trigonal bipyramid ($\tau = 0.17$).⁵⁰ The apex of the square pyramid is occupied by one of the bromide ligands with a Cu–Br1 bond length of 2.8517(4) Å. This is significantly longer than the distances to the two remaining Br ligands which together with the two nitrogen donors constitute the basal plane (Cu–Br2: 2.4260(3) Å, Cu–Br3: 2.4268(3) Å).

Determination of Formation Constants. Formation of $\text{Me}_3\text{tach}^{19}$ complexes in aqueous media was studied by potentiometric methods. Owing to the high rigidity of the ligand, complex formation was slow, and the stability constants could often not be determined by means of continuous titrations. Only metal cations displaying particularly fast ligand exchange kinetics such as Cu^{II} and Zn^{II} could be studied by this method. The results of these experiments are collected in Table 5. Both metal cations form the expected simple ML^{2+} and ML_2^{2+} complexes as major components. In particular, the stability of the *mono*-complexes ML^{2+} is remarkably high. Cu^{II} forms a

(47) (a) Evans, D. F. *J. Chem. Soc.* **1959**, 2003. (b) Corsi, D. M.; Platas-Iglesias, C.; van Bekkum, H.; Peters, J. A. *Magn. Reson. Chem.* **2001**, *39*, 723.

(48) Bortoluzzi, A. J.; Neves, A.; Terra, G. G. *Acta Crystallogr., Sect. E* **2006**, *62*, m2965.

(49) (a) Hegetschweiler, K.; Gramlich, V.; Ghisletta, M.; Samaras, H. *Inorg. Chem.* **1992**, *31*, 2341. (b) Reiss, G. J.; Frank, W.; Hegetschweiler, K.; Kuppert, D. *Acta Crystallogr., Sect. C* **1998**, *54*, 614.

(50) Addison, A. W.; Rao, T. N.; Reedijk, J.; van Rijn, J.; Verschoor, G. C. *J. Chem. Soc., Dalton Trans.* **1984**, 1349.

protonated *mono*-complex $[M(\text{HL})]^{3+}$ which appears as a minor species in acidic media. Its abundance never exceeds 10%. Zn^{II} does not form an analogous protonated complex. For both metal cations a deprotonation of the *mono*-complex was observed. We tentatively formulate the resulting species as hydroxo complexes with *bis-μ*-hydroxo bridging for the binuclear $[\text{LM}(\mu\text{-OH})_2\text{-ML}]^{2+}$.^{49a}

Formation of MeL^{a} complexes with Mn^{II} , Co^{II} , Ni^{II} , Cu^{II} , Zn^{II} , and Cd^{II} was studied by the same method (Table 6) in 0.1 M KCl at 25 °C. In addition, the $\text{Cd}^{\text{II}}\text{-MeL}^{\text{a}}$ system has been investigated in a 0.1 M KNO_3 medium. In our previous paper, reporting the coordination chemistry of L^{a} ,¹⁰ we have not yet studied formation constants of $\text{Mn}^{\text{II}}\text{-L}^{\text{a}}$ complexes; for the sake of comparability, they have now been determined as well, and are included in Table 6. The $\text{Cu}^{\text{II}}\text{-MeL}^{\text{a}}$ and $\text{Ni}^{\text{II}}\text{-MeL}^{\text{a}}$ system was also investigated in 1 M KCl or 1 M KNO_3 , and metal complex formation was additionally followed by Vis spectroscopic measurements. The Vis data was used to double-check the evaluated formation constants (Supporting Information, Table S4); it also allowed the calculation of an individual spectrum for each species (Supporting Information, Figure S5). Complete equilibration was always verified by performing back-titrations, but in contrast to the above-mentioned Me_3tach , complex formation with MeL^{a} was generally found to be fast. This was even the case for Ni^{II} in an acidic medium, where complex formation with several other cyclic triamine ligands has been reported to be sluggish.^{5a,7,16,49a} In general, the main species formed in solution are the *mono*- and the *bis*-complex $[\text{M}(\text{MeL}^{\text{a}})]^{2+}$ and $[\text{M}(\text{MeL}^{\text{a}})_2]^{2+}$.

Table 5. Formation Constants ($\log \beta_{xyz}$)^a of 2,4,6- Me_3tach (= L) Complexes (25 °C, $I = 0.1$ M KCl)

Complex, $\log \beta_{xyz}$ ^a	Cu^{II}	Zn^{II}
$[\text{ML}]^{2+}$, $\log \beta_{110}$	16.27(1)	12.62(1)
$[\text{M}(\text{HL})]^{3+}$, $\log \beta_{111}$	19.00(8)	
$[\text{ML}(\text{OH})]^{+}$, $\log \beta_{11-1}$		3.90(5)
$[\text{ML}(\text{OH})_2]$, $\log \beta_{11-2}$		-7.56(6)
$[\text{M}_2\text{L}_2(\text{OH})_2]^{2+}$, $\log \beta_{22-2}$	19.26(3)	10.89(8)
$[\text{ML}_2]^{2+}$, $\log \beta_{120}$	26.97(5)	21.98(3)

^a $\beta_{xyz} = [\text{M}_x\text{L}_y\text{H}_z] \times [\text{M}]^{-x} \times [\text{L}]^{-y} \times [\text{H}]^{-z}$. The uncertainties given in parentheses correspond to 3σ .

Table 6. Formation Constants ($\log \beta_{xyz}$)^a of L^{a} and MeL^{a} (= L) Complexes (25 °C, $I = 0.1$ M KCl, unless Otherwise Noted)

	$[\text{M}^{\text{II}}\text{L}]^{2+}$	$[\text{M}^{\text{II}}(\text{HL})]^{3+}$	$[\text{M}^{\text{II}}(\text{L})\text{H}_{-1}]^{+}$	$[\text{M}^{\text{II}}(\text{L})_2\text{H}_{-1}]^{+}$	$[\text{M}^{\text{II}}\text{L}_2]^{2+}$	$[\text{M}^{\text{II}}(\text{L})(\text{HL})]^{3+}$
	$\log \beta_{110}$	$\log \beta_{111}$	$\log \beta_{11-1}$	$\log \beta_{12-1}$	$\log \beta_{120}$	$\log \beta_{121}$
$\text{L} = \text{L}^{\text{a}}$						
Mn	3.26(1)		-7.16(4)	-4.6(1)	5.0(3)	
$\text{L} = \text{MeL}^{\text{a}}$						
Mn	3.99(2)	11.17(9)		-2.43(4)	7.08(8)	
Co	8.48(5)	12.8(2)			16.75(4)	21.5(3)
Ni	11.34(2) ^b	14.1(2)		11.11(6)	22.07(3) ^c	
Cu	11.96(1)	14.99(4)	4.63(2)		22.16(2)	25.5(3)
Zn	8.14(6)			4.30(7)	15.65(2)	20.6(2)
Cd^d	7.03(1)	12.02(5)			12.72(2)	19.21(6)
Cd^e	7.03(1)				13.33(1)	19.18(7)

^a $\beta_{xyz} = [\text{M}_x\text{L}_y\text{H}_z] \times [\text{M}]^{-x} \times [\text{L}]^{-y} \times [\text{H}]^{-z}$. The uncertainties given in parentheses correspond to 3σ . ^b Reference 8 reports a value of 11.39 (aqueous solution, 25 °C, ionic strength not specified). ^c Reference 8 reports a value of 6.54 (aqueous solution, 25 °C, ionic strength not specified). ^d 0.1 M KCl; conditional constants (chloro complex formation), see text. ^e 0.1 M KNO_3 .

Additionally, the protonation products $[\text{M}(\text{HMeL}^{\text{a}})]^{3+}$ or $[\text{M}(\text{HMeL}^{\text{a}})(\text{MeL}^{\text{a}})]^{3+}$, and deprotonated species such as $[\text{M}(\text{MeL}^{\text{a}})\text{H}_{-1}]^{+}$ or $[\text{M}(\text{MeL}^{\text{a}})_2\text{H}_{-1}]^{+}$ were detected. The deprotonation products may again be regarded as hydroxo-complexes. $[\text{M}(\text{MeL}^{\text{a}})(\text{OH})]^{+}$ formation corresponds simply to the deprotonation of a coordinated water molecule. Formation of $[\text{M}(\text{MeL}^{\text{a}})_2(\text{OH})]^{+}$, however, implies either an increase of the coordination number to 7 or a bidentate coordination for one of the MeL^{a} ligands.

Compared to the parent L^{a} , the methylated MeL^{a} forms complexes of slightly higher stability. The close similarity of L^{a} and MeL^{a} can be expressed in terms of linear free energy relations (Figure 7):

$$\log \beta_{110}(\text{MeL}^{\text{a}}) = 1.02(2) \cdot \log \beta_{110}(\text{L}^{\text{a}}) + 0.53(14) \quad (1)$$

$$\log \beta_{120}(\text{MeL}^{\text{a}}) = 0.98(3) \cdot \log \beta_{120}(\text{L}^{\text{a}}) + 1.8(4) \quad (2)$$

A few other features which follow from our equilibrium study should be mentioned here briefly; they have already been discussed in more detail for the analogous L^{a} derivatives in our previous paper:

- the rather low stability of the *mono*-complexes $[\text{M}^{\text{II}}(\text{MeL}^{\text{a}})]^{2+}$; and
- the comparably high tendency for forming *bis*-complexes.
- An inversion of the Irving-Williams order in the reaction $\text{M}(\text{MeL}^{\text{a}})^{2+} + \text{MeL}^{\text{a}} \rightleftharpoons \text{M}(\text{MeL}^{\text{a}})_2^{2+}$ with $\log K = 10.73$ for Ni^{II} , but only 10.20 for Cu^{II} . As is well-known, facially coordinating cyclic triamines have a reduced tendency to bind Jahn–Teller active metal centers.^{7,10,16,49a}
- The blue-shift observed upon protonation of $[\text{Cu}(\text{MeL}^{\text{a}})_2]^{2+}$. A λ_{max} of 565 nm observed for $[\text{Cu}(\text{HMeL}^{\text{a}})(\text{MeL}^{\text{a}})]^{3+}$ (Supporting Information, Table S4 and Figure S5) is indicative of a tetragonal CuN_4 chromophore⁵¹ suggesting thus a bidentate coordination of both ligand entities.
- The ${}^3\text{A}_{2g} - {}^3\text{T}_{1g}(\text{F})$ transition of $[\text{Ni}(\text{MeL}^{\text{a}})]^{2+}$ and $[\text{Ni}(\text{MeL}^{\text{a}})_2]^{2+}$, which is observed at 595 and 518 nm, respectively. Both observations are in agreement with an octahedral triamine-triaqua- Ni^{II} and hexaamine- Ni^{II} chromophore (see also the

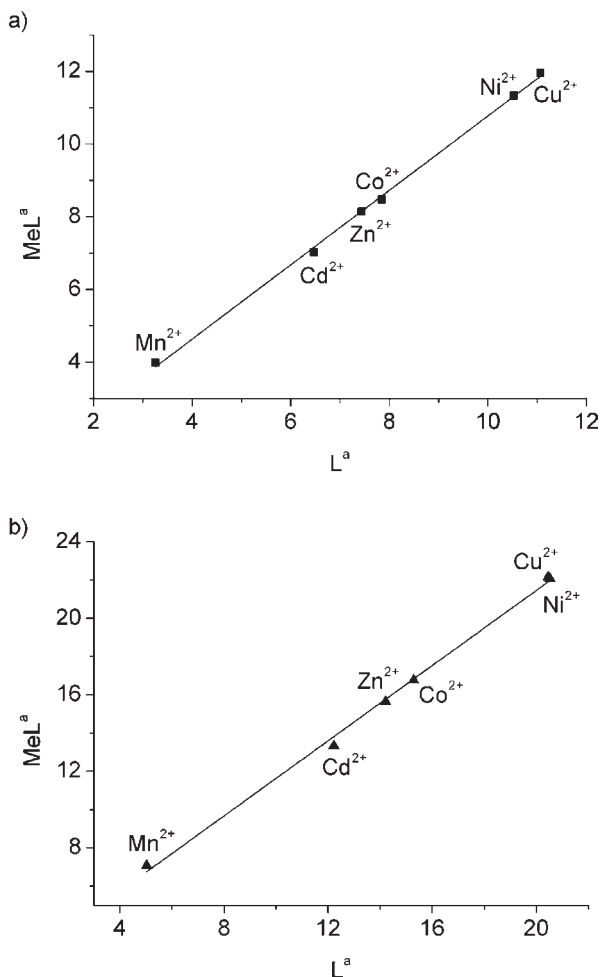


Figure 7. Linear free energy relations for (a) $\log \beta_{110}$ (eq 1) and (b) $\log \beta_{120}$ (eq 2) of the $[ML]^{2+}$ and $[ML_2]^{2+}$ complexes for $L = L^a$ and MeL^a ($M = Mn^{II}, Cd^{II}, Zn^{II}, Co^{II}, Ni^{II}, Cu^{II}$). $\beta_{1,0} = [ML_x] \times [M]^{-1} \times [L]^{-x}$; the explicit values are listed in the Supporting Information, Table S6. The data for Cd refer to the 0.1 M KNO_3 medium.

crystal structure of $[Ni(MeL^a)_2](ClO_4)_2$ reported by Peralta et al.).^{8,10}

- (f) Chloro complex formation in the KCl media. It has frequently been discussed that the affinity of Cd^{II} for Cl^- is sufficiently high to form chloro complexes such as $[CdCl]^+$,^{7,10,23} but also $[Cd(MeL^a)Cl]^+$ (see also the solid state structure of **4**). Consequently, the formation constants determined in 0.1 M KCl (Table 6) must be considered as conditional constants. It is noteworthy that $\log \beta_{110}$ evaluated for the 0.1 M KCl and the 0.1 M KNO_3 medium is equal within significance. If one accepts that the value in 0.1 M KNO_3 corresponds to the true formation constant (negligible NO_3^- binding), and that the activity coefficients are solely dependent on ionic strength, one can deduce an equally strong binding of Cl^- to Cd^{2+} and to $[Cd(MeL^a)]^{2+}$. The significantly higher value of $\log \beta_{120}$ in the 0.1 M KNO_3 medium compared to the 0.1 M KCl medium indicates an absence of a direct binding of Cl^- to the *bis*-complex

Table 7. Half Cell Potentials ($E_{1/2}$, Relative to NHE) Obtained from Cyclic Voltammetry for $[M(MeL^a)_2]^{3+/2+}$, $[M(L^a)_2]^{3+/2+}$, and $[M(dapi)_2]^{3+/2+}$ Couples in Aqueous Solution

$[ML_2]^{3+/2+}$	$E_{1/2}$ [V]
$[Co(MeL^a)_2]^{3+/2+}$	-0.24 ^{a,b}
$[Co(L^a)_2]^{3+/2+}$	-0.21 ^{c,d}
$[Co(dapi)_2]^{3+/2+}$	-0.38 ^c
$[Fe(MeL^a)_2]^{3+/2+}$	0.24 ^a
$[Fe(dapi)_2]^{3+/2+}$	0.09 ^a
$[Ni(MeL^a)_2]^{3+/2+}$	1.02, ^{a,e}
$[Ni(L^a)_2]^{3+/2+}$	1.04 ^c
$[Ni(dapi)_2]^{3+/2+}$	0.92 ^c

^aThis work. ^b*trans*- $[Co(MeL^a)_2]^{3+}$ or $CoCl_2/MeL^a$ as starting material. ^cReference 10. ^dNo difference was observed for solutions using the *cis*- or *trans*-isomer of $[Co(L^a)_2]^{3+}$ as starting material; see also reference 10. ^eReference 8 reports a value of 1.05 V.

$[Cd(MeL^a)_2]^{2+}$. A quantitative evaluation of such Cl^- -binding is possible; the result is provided in the Supporting Information, Figure S6, Table S5. Similarly, some weak binding of Cl^- to Cu^{2+} must be considered in the 1.0 M KCl medium (see again the Supporting Information, Table S5).

Redox Properties. The redox potentials of $[M(MeL^a)_2]^{3+/2+}$ ($M = Fe, Co, Ni$) and, for comparison, of $[Fe(dapi)_2]^{3+/2+}$ were determined by cyclic voltammetry. The analysis of the experimental data generally revealed quasi-reversible electron transfer for these redox couples (Table 7). In all cases, the peak current was found to depend linearly on the square root of the scan rate, indicative of a diffusion controlled electron transfer. At slow scan rates, the cathodic peak current of the $[Fe(MeL^a)_2]^{3+/2+}$ system was found to be significantly reduced, and this effect increased with decreasing scan rate. For a scan rate of 1000 mV s^{-1} the ratio of the anodic to the cathodic peak current was unity, whereas for 5 mV s^{-1} this ratio reached a value of 1.4. We explain this observation by a slow hydrolysis of $[Fe(MeL^a)_2]^{3+}$. Notably, such a behavior has not been observed for $[Fe(dapi)_2]^{3+/2+}$. The redox potential of the $[Co(MeL^a)_2]^{3+/2+}$ -couple can be used to estimate the formation constants of the inert $[Co^{III}(MeL^a)_2]^{3+}$ complex as $\log \beta_{120} \approx 52$.

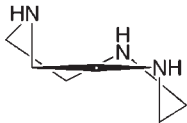
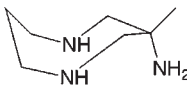
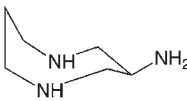
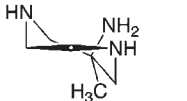
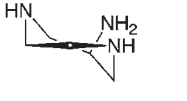
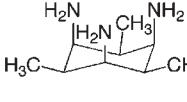
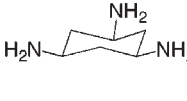
The redox potentials of the L^a - and MeL^a -complexes are very similar, whereas the redox potentials of corresponding dapi complexes are slightly more negative (less positive). This finding is in agreement with the favored binding of the smaller cation by six-membered chelate rings.⁵² The term $\Delta E_{1/2} = E_{1/2}[M(dapi)_2]^{3+/2+} - E_{1/2}[M(MeL^a)_2]^{3+/2+} = -RTF^{-1} \{ \ln[\beta_2^{III}(dapi)/\beta_2^{II}(dapi)] - \ln[\beta_2^{III}(MeL^a)/\beta_2^{II}(MeL^a)] \} = -RTF^{-1} \Delta \ln(\beta_2^{III}/\beta_2^{II})$, where β_2^{III} and β_2^{II} stand for the formation constants of $[M^{III}(L)]^{3+}$ and $[M^{II}(L)]^{2+}$, respectively, can be regarded as a quantitative measure of this effect. For Fe, Co, and Ni, $\Delta \log(\beta_2^{III}/\beta_2^{II})$ is 2.5, 2.4, and 1.7, respectively.

Molecular Modeling Calculations. Molecular mechanics calculations have been performed to elucidate the difference in strain energy for the free ligand and a corresponding complex. The following triamine ligands with a cyclic backbone have been considered (Chart 1): the cyclohexane-based tach and 2,4,6- Me_3 tach, the 1,4-diazacycloheptane based L^a and MeL^a , the 1,4-diaza-cyclooctane based L^b and MeL^b and 1,4,7-triaza-cyclononane

(51) (a) Prenesti, E.; Daniele, P. G.; Prencipe, M.; Ostacoli, G. *Polyhedron* **1999**, *18*, 3233. (b) Zimmer, A.; Kuppert, D.; Weyhermüller, T.; Müller, I.; Hegetschweiler, K. *Chem.—Eur. J.* **2001**, *7*, 917.

(52) Hancock, R. D. *Acc. Chem. Res.* **1990**, *23*, 253.

Table 8. Strain Energies (kJ mol⁻¹) of Some Triamine Ligands and Its Co^{III} Complexes

	Bond Def.	Valence Angle Def.	Torsion Angle Def.	Non-Bond. Interactions	Total Strain	
	tacn	1.06	7.37	10.96	12.58	31.98
	[CoL(H ₂ O) ₃] ³⁺	4.56	6.80	18.90	25.32	55.59
	[CoL(NH ₃) ₃] ³⁺	8.99	5.51	19.86	33.17	67.53
	[CoL ₂] ³⁺	11.65	10.27	39.73	43.93	105.59
	$\Delta E^1, \Delta E^2, \Delta E^3$	23.61, ^a	35.55, ^b	41.63 ^c		
	MeL ^b	2.06	7.62	7.52	20.13	37.23
	[CoL(H ₂ O) ₃] ³⁺	5.76	15.13	11.56	33.78	66.23
	[CoL(NH ₃) ₃] ³⁺	10.97	16.09	11.35	43.37	81.77
	[CoL ₂] ³⁺	16.15	29.57	22.93	67.00	135.65
	$\Delta E^1, \Delta E^2, \Delta E^3$	29.00, ^a	44.54, ^b	61.19 ^c		
	L ^b	1.39	7.81	7.45	15.92	32.57
	[CoL(H ₂ O) ₃] ³⁺	5.56	14.55	11.45	31.32	62.89
	[CoL(NH ₃) ₃] ³⁺	10.73	16.06	11.23	40.59	78.61
	[CoL ₂] ³⁺	15.82	29.36	22.66	61.38	129.22
	$\Delta E^1, \Delta E^2, \Delta E^3$	30.32, ^a	46.04, ^b	64.08 ^c		
	MeL ^a	1.72	8.98	7.46	16.93	35.09
	[CoL(H ₂ O) ₃] ³⁺	4.94	10.23	20.43	31.17	66.77
	[CoL(NH ₃) ₃] ³⁺	9.04	10.67	20.42	39.01	79.14
	[CoL ₂] ³⁺	10.49	19.09	40.60	54.60	124.78
	$\Delta E^1, \Delta E^2, \Delta E^3$	31.68, ^a	44.05, ^b	54.60 ^c		
	L ^a	1.00	8.97	7.16	12.61	29.74
	[CoL(H ₂ O) ₃] ³⁺	4.68	10.21	20.33	28.74	63.96
	[CoL(NH ₃) ₃] ³⁺	8.80	10.63	20.32	36.52	76.29
	[CoL ₂] ³⁺	10.12	18.98	40.41	49.54	119.05
	$\Delta E^1, \Delta E^2, \Delta E^3$	34.22, ^a	46.55, ^b	59.57 ^c		
	2,4,6-Me ₃ tach	4.09	11.77	0.95	28.04	44.85
	[CoL(H ₂ O) ₃] ³⁺	7.37	14.85	2.09	43.11	67.41
	[CoL(NH ₃) ₃] ³⁺	12.74	15.57	2.04	52.16	82.51
	[CoL ₂] ³⁺	18.94	34.53	1.68	82.98	138.12
	$\Delta E^1, \Delta E^2, \Delta E^3$	22.56, ^a	37.66, ^b	48.42 ^c		
	tach	1.36	1.31	0.32	16.60	19.59
	[CoL(H ₂ O) ₃] ³⁺	5.35	7.36	1.33	33.27	47.32
	[CoL(NH ₃) ₃] ³⁺	10.82	8.38	1.26	42.41	62.98
	[CoL ₂] ³⁺	15.38	18.58	2.22	63.84	100.03
	$\Delta E^1, \Delta E^2, \Delta E^3$	27.73, ^a	43.39, ^b	60.85 ^c		

$$^a \Delta E^1 = E\{\text{[Co(L)(H}_2\text{O)}_3\text{]}^{3+}\} - E(\text{L}).$$

$$^b \Delta E^2 = E\{\text{[Co(L)(NH}_3\text{)}_3\text{]}^{3+}\} - E(\text{L}).$$

$$^c \Delta E^3 = E\{\text{[Co(L)}_2\text{]}^{3+}\} - 2E(\text{L}).$$

(tacn). Molecular mechanics calculations have frequently been misused in coordination chemistry.³⁴ To avoid possible pitfalls in the interpretation,⁵³ the calculated strain energies E of the free ligands, the *mono*-complexes [Co(L)(H₂O)₃]³⁺ and [Co(L)(NH₃)₃]³⁺, and the *bis*-complexes [Co(L)₂]³⁺ were combined to $\Delta E^1 = E\{\text{[Co(L)(H}_2\text{O)}_3\text{]}^{3+}\} - E\{\text{L}\}$, $\Delta E^2 = E\{\text{[Co(L)(NH}_3\text{)}_3\text{]}^{3+}\} - E\{\text{L}\}$, and $\Delta E^3 = E\{\text{[Co(L)}_2\text{]}^{3+}\} - 2E\{\text{L}\}$. These quantities can

(53) Steric strain in a molecule generally increases with an increasing number of atoms and a direct comparison of the amount of strain should only be made for isomers. Moreover, the calculated amount of strain for different *constitutional* isomers has sometimes been mistaken as a measure for the enthalpy of formation, which is obviously wrong as illustrated by the trivial example of 1,2-ethanediol and dimethylperoxide, two constitutional isomers with a similarly low amount of strain but a very different ΔH^f . Furthermore, one must consider that force fields are generally optimized to fit structural parameters rather than energies. Since quantum mechanical calculations for medium sized molecules do not represent a major challenge nowadays, one may (and several scientists actually did) consider molecular mechanics calculations as outdated. The persuasive advantage of this method is, however, the possibility for an easy location and identification of the various types of strain (such as non-bonding interactions, torsional strain, or bond- and angle deformation) concretely in the molecular structure.

be regarded as a direct measure of the *increase* in strain on complex formation for a particular ligand L.

The results of these calculations are shown in Table 8, and can be summarized as follows:

- Regarding formation of the *mono*-complexes, the ligands considered can be grouped into two classes: For Me₃tach and tacn, the increase in strain upon complex formation is comparably low ($\Delta E^1 = 23\text{--}24$ kJ mol⁻¹, $\Delta E^2 = 36\text{--}38$ kJ mol⁻¹). The other five ligands show significantly higher values ($\Delta E^1 = 28\text{--}34$ kJ mol⁻¹, $\Delta E^2 = 43\text{--}47$ kJ mol⁻¹). This behavior is also observed for the *bis*-complexes (Me₃tach, tacn: $\Delta E^3 = 42\text{--}48$ kJ mol⁻¹, other ligands: $55\text{--}64$ kJ mol⁻¹), although the *bis*-complex of Me₃tach is considerably more destabilized than the corresponding tacn derivative. The relatively high amount of strain in *bis*-complexes of ligands with an all-*cis*-cyclohexane-1,3,5-triamine framework has previously been discussed in terms of particularly unfavorable non-bonding interligand interactions between the

N–H hydrogen atoms.⁵⁴ This effect is clearly expressed in the table by the high amount of non-bonding interactions for $[\text{Co}(\text{tach})_2]^{3+}$ (64 kJ mol^{-1}) and $[\text{Co}(\text{Me}_3\text{tach})_2]^{3+}$ (83 kJ mol^{-1}).

- (ii) The free tach ligand, having the three amino groups in equatorial position, requires a significant amount of energy to reach the triaxial conformation required for metal binding. For the free Me_3tach (and even for the doubly protonated $\text{H}_2\text{Me}_3\text{tach}^{2+}$), the most stable conformer already has three axial amino groups. The donor set of Me_3tach is therefore much better preorganized. This is clearly shown by $\Delta\Delta E^1 = \Delta E^1(\text{tach}) - \Delta E^1(\text{Me}_3\text{tach}) = 5.2 \text{ kJ mol}^{-1}$, $\Delta\Delta E^2 = 5.7 \text{ kJ mol}^{-1}$, and $\Delta\Delta E^3 = 12.4 \text{ kJ mol}^{-1}$. A much weaker effect is observed for L^a/MeL^a ($\Delta\Delta E^1 = 2.5 \text{ kJ mol}^{-1}$, $\Delta\Delta E^2 = 2.5 \text{ kJ mol}^{-1}$, and $\Delta\Delta E^3 = 5.0 \text{ kJ mol}^{-1}$) and L^b/MeL^b ($\Delta\Delta E^1 = 1.3 \text{ kJ mol}^{-1}$, $\Delta\Delta E^2 = 1.5 \text{ kJ mol}^{-1}$, and $\Delta\Delta E^3 = 2.9 \text{ kJ mol}^{-1}$). In terms of ligand design, one can thus state that the addition of the three methyl groups to tach resulted in an ideal preorientation of the donor set, whereas L^a and L^b do not benefit in the same extent from the introduction of an additional methyl group. These considerations are clearly reflected in the stability constants. From the ligands under consideration, tach forms the weakest, Me_3tach the strongest ML-complexes with divalent transition metal cations.
- (iii) It has already been noted that the stability of $\text{M}(\text{L}^a)$ and $\text{M}(\text{MeL}^a)$ *mono*-complexes is surprisingly low. Inspection of Table 8 explains this finding as a consequence of the considerable amount of torsional strain, which is present in the complexes, but not in the free ligand. The torsional strain can explicitly be located in the eclipsed conformation of the $\text{NH}-\text{CH}_2-\text{CH}_2-\text{NH}$ fragment. It is noteworthy that *tacn* complexes also exhibit an appreciable amount of torsional strain; however, this strain is to a significant amount already preformed in the free ligand,⁵⁵ and the increase of torsional strain upon complex formation is thus relatively minor.
- (iv) Ion size effects: The adamantane-type structure of an $\text{M}(\text{tach})$ or $\text{M}(\text{Me}_3\text{tach})$ fragment comprises three fused, six-membered chelate rings. For a very small metal cation M, having a size comparable to a carbon atom, these rings would adopt an ideal chair conformation, and the entire structure would be devoid of any angle-deformation- or torsional strain.⁵⁴ Increasing ion size induces some additional valence angle deformation; the torsional strain, however, remains low. For L^a and MeL^a the situation turns out to be the reverse. The exclusive formation of five membered chelate rings is an advantage for the accommodation of large metal cations.⁵² Moreover, the above-

mentioned torsional strain within the N–C–N fragment also shows a dependence on the metal ion size. To elucidate this effect, calculations were performed where the ion radius was varied systematically. It must be emphasized that such calculations are not straightforward, because a force field for such a generalized metal ion is not per se defined. To minimize the influence of a specific force field, the calculations were performed for two different setups. In a first case, the force field of Co^{III} was used, implying though an octahedral coordination with explicit N–Co–N angle deformation and relatively high force constants for Co–N bond stretching. In a second approach, the force field of Zn^{II} was used with a much smaller force constant for Zn–N bond stretching and no strain for N–Zn–N angle deformation (in this case, the coordination geometry around the metal cation is solely modeled by non-bonding interactions between the coordinated donor atoms). Although some differences were noted for the two setups, the same qualitative picture, displaying a sigmoid shape of the strain energy curve as a function of ion size, was observed: For small metal cations up to an M–N bond distance of about 2.2 Å, the N–C–N torsion angle remains approximately constant close to zero ($<3^\circ$). In the range 2.2–2.4 Å, a significant increase of the N–C–N angle is observed, the precise location of the ascent considerably depended on the type of force field used. For very large cations with an M–N bond distance longer than 2.4 Å, the N–C–N angle remains again approximately constant at a value of about $22\text{--}26^\circ$. The available crystal structure data for MeL^a complexes (Table 4) showed indeed very small torsional N–C–N angles for all complexes with a first-row transition metal cation. For Cd^{II} , this value is slightly increased. We do not have data for MeL^a complexes with very large metal cations; however, a series of Sc^{III} and Y^{III} complexes with N-alkylated derivatives of MeL^a have recently been reported.⁵⁶ In these complexes with M–N distances up to 2.4–2.8 Å, the N–C–N torsional angles do indeed fall in the range of $24\text{--}26^\circ$. It must be emphasized that such a value is still closer to an eclipsed than to a staggered conformation. However, it becomes clear that for large metal ions some of the torsional strain is released.

Discussion

If triamine units with a cyclic structure (Chart 1) are considered as scaffolds for tailored chelating agents, it is of importance to account for the specific steric requirements of the ligand backbones. In this paper, we have shown that different cyclic triamines may display significant differences in metal binding. Our analysis is based on structural and stability data of *dapi*, Me_3tach ,¹⁹ L^a and MeL^a complexes,

(54) Hegetschweiler, K.; Hancock, R. D.; Ghisletta, M.; Kradolfer, T.; Gramlich, V.; Schmalte, H. W. *Inorg. Chem.* **1993**, *32*, 5273.

(55) (a) McDougall, G. J.; Hancock, R. D.; Boeyens, J. C. A. *J. Chem. Soc., Dalton Trans.* **1978**, 1438. (b) Thöm, V. J.; Boeyens, J. C. A.; McDougall, G. J.; Hancock, R. D. *J. Am. Chem. Soc.* **1984**, *106*, 3198. (c) Hancock, R. D.; Martell, A. E. *Comments Inorg. Chem.* **1988**, *6*, 237.

(56) (a) Ge, S.; Bambirra, S.; Meetsma, A.; Hessen, B. *Chem. Commun.* **2006**, 3320. (b) Ge, S.; Meetsma, A.; Hessen, B. *Organometallics* **2007**, *26*, 5278. (c) Ge, S.; Meetsma, A.; Hessen, B. *Organometallics* **2008**, *27*, 5339. (d) Ge, S.; Meetsma, A.; Hessen, B. *Organometallics* **2009**, *28*, 719.

and on molecular mechanics calculation for some complexes and free ligands. The relatively poor chelating properties of the tach ligand are well-known and have been interpreted in a “wrong”, equatorial arrangement of the amino groups.^{5a} The efficiency in metal chelation can be increased considerably by furnishing the tach skeleton with additional substituents, which help stabilizing a triaxial form of the donor set. Our investigation fully confirms the assumption proposed in the introduction: in comparison to the trihydroxy and trimethoxy derivatives,⁵⁷ the increased steric demand of the methyl groups⁵⁸ resulted in a further increase of stability. As we have shown, even the doubly protonated $\text{H}_2\text{Me}_3\text{tach}^{2+}$ retains a chair conformation with axial nitrogen atoms. Moreover, the electronegative oxygen atoms of the hydroxy or methoxy groups reduce the nucleophilicity of the amino groups. As a consequence the methylated ligands are stronger bases and form once more complexes of higher stability. Regarding formation of *mono*-complexes $[\text{M}^{\text{II}}\text{L}]^{2+}$ with late divalent transition metal cations, Me_3tach even surpasses *tacn* and obviously represents one of the most effective tridentate chelators for divalent transition metal cations known to date (Figure 8).

Similar to the simple tach, the 1,4-diazepan-6-amine unit L^{a} forms in general *mono*-complexes of a remarkably low stability. One may again consider, whether the preorganization of the donor set could be improved by adding an additional methyl group to the cyclic framework, which would help to bring the amino group in an axial position. However, in contrast to Me_3tach , MeL^{a} shows only a weak gain in stability in comparison to the parent L^{a} . This is clearly expressed by the linear free energy relations 1 and 2 for *mono*- and *bis*-complexes which are strictly obeyed for divalent transition metal cations. The rather low stability of these complexes follows in fact from the unfavorable eclipsed orientation within the $\text{HN}-\text{CH}_2-\text{CH}_2-\text{NH}$ fragment. This geometry is only enforced in the tridentate coordination mode, and the detachment of one of the endocyclic amino groups from the metal cation resulted in a considerable release of torsional strain. In this investigation we have amply provided experimental evidence for these considerations:

- The high tendency for forming partially protonated complexes such as $[\text{MHL}]^{3+}$ and $[\text{ML}(\text{HL})]^{3+}$. Protonation of coordinated polyamine ligands in an acidic medium is in general well established.⁵⁹ However, for L^{a} and MeL^{a} the amount of protonation is unusual. This is particularly true for the $\text{Cu}^{\text{II}}-\text{MeL}^{\text{a}}$ system, where $[\text{Cu}(\text{HMeL}^{\text{a}})]^{3+}$ was found to be a major species at an ionic strength of 1 M (Figure 9). Formation of a corresponding $[\text{Cu}(\text{Me}_3\text{tach})(\text{HMe}_3\text{tach})]^{3+}$ has not been observed, and $[\text{Cu}(\text{HMe}_3\text{tach})]^{3+}$ is a minor species which is formed at most to an extent of < 10% at $\text{pH} < 4$.
- We have succeeded in crystallizing the $[\text{Cu}(\text{HMeL}^{\text{a}})]^{3+}$ species as a bromo complex from a slightly acidic aqueous medium. Inspection of the

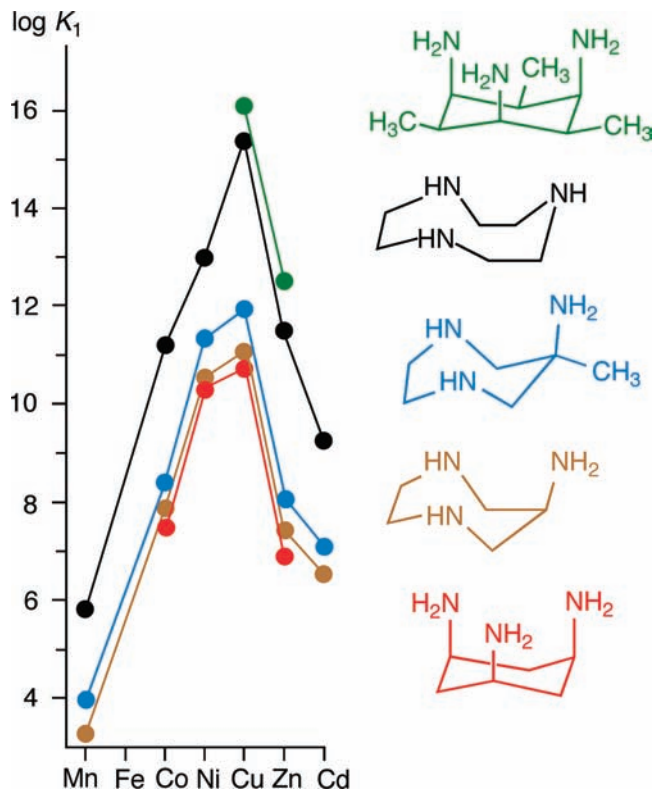


Figure 8. Survey of formation constants $K_1 = [\text{ML}][\text{M}]^{-1}[\text{L}]^{-1}$ for complexes with divalent cations and various cyclic triamine ligands as indicated. The values are from this work (Me_3tach , L^{a} and MeL^{a} : Tables 5 and 6), from reference 10 (L^{a}) and from reference 28 (*tacn* and *tach*).

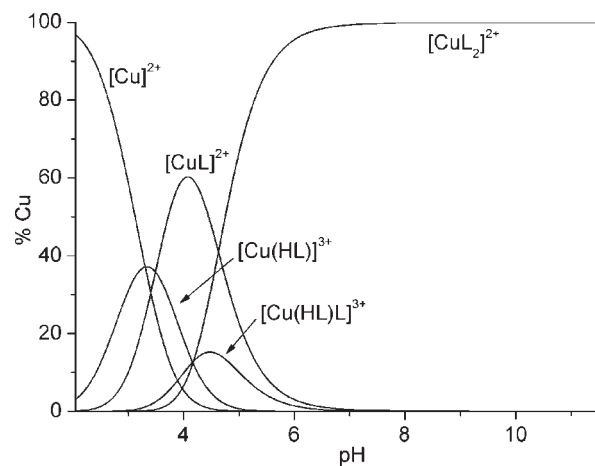


Figure 9. Species distribution plots for the $\text{Cu}^{\text{II}}-\text{MeL}^{\text{a}}$ system in aqueous solution (25 °C, 1.0 M KCl) calculated for total Cu = 1 mM, total MeL^{a} = 2 mM, using the formation constants (potentiometric titration) listed in Supporting Information, Table S4.

crystal structure established an $\text{N}-\text{C}-\text{C}-\text{N}$ torsional angle of 69.7° , reaching closely the needs for a completely relaxed 60° arrangement.

- It is clear that formation of such protonated complexes is a direct proof for a bidentate coordination of the MeL^{a} ligand. However, the spectrophotometric data also provided evidence that even the fully deprotonated ligand may sometimes coordinate in a bidentate rather than a tridentate fashion: $[\text{Cu}(\text{MeL}^{\text{a}})(\text{HMeL}^{\text{a}})]^{3+}$ absorbs at $\lambda_{\text{max}} = 565 \text{ nm}$,

(57) Hegetschweiler, K. *Chem. Soc. Rev.* **1999**, 28, 239.

(58) Eliel, E. L.; Wilen, S. H. *Stereochemistry of Organic Compounds*; John Wiley: New York, 1994.

(59) (a) Paoletti, P.; Walser, R.; Vacca, A.; Schwarzenbach, G. *Helv. Chim. Acta* **1971**, 54, 243. (b) Bianchi, A.; Micheloni, M.; Paoletti, P. *Coord. Chem. Rev.* **1991**, 110, 17. (c) Gramlich, V.; Lubal, P.; Musso, S.; Anderegg, G. *Helv. Chim. Acta* **2001**, 84, 623. (d) Blackman, A. G. C. *R. Chim.* **2005**, 8, 107.

a value which fits to a tetragonal *trans*-CuN₄ chromophore. A Cu^{II}-pentaamine chromophore would have a maximum at > 600 nm (see [Cu^{II}(HL)]³⁺, L = *bis*-taci or 4,7-*bis*(2-aminoethyl)-1,4,7,10-tetraazadecane).^{23,59c}

All these experimental findings are further corroborated⁶⁰ by the molecular mechanics calculations which revealed high torsional strain for L^a and MeL^a complexes.

As we became aware of the torsional destabilization of L^a and MeL^a complexes, we thought that an expansion of the diaminoethylene- to a diaminopropylene-fragment by inserting an additional methylene group would help to release torsional strain and could result in higher complex stability. Molecular mechanics calculation for the corresponding 1,5-diazocan-3-amine L^b indeed revealed an approximately *gauche* conformation throughout the diamino-cyclooctane ring with a correspondingly low amount of torsional strain. However, the calculated increase in total strain energy ($\Delta E^1 = 30 \text{ kJ mol}^{-1}$, $\Delta E^2 = 46 \text{ kJ mol}^{-1}$, $\Delta E^3 = 64 \text{ kJ mol}^{-1}$) remains relatively high because of a high amount of valence angle deformation and unfavorable non-bonding interactions. Similar to L^a, addition of a methyl group to L^b, intending to improve preorganization of the donor set, only resulted in a minor decrease of ΔE^1 , ΔE^2 , or ΔE^3 , and in analogy to MeL^a-complexes, MeL^b-derivatives, must also be regarded as significantly strained.

To get back to the opening question:⁸ “*Can MeL^a act as a mimetic ligand for tacn?*” The answer is a limited yes if one regards for instance the similar size effects in accommodating metal ions. MeL^a and tacn both form exclusively five-membered chelate rings and have thus a preference in binding large metal cations. This is different for the cyclohexane-based systems such as tach, dapi, taci, tmca, or Me₃tach. There is also some similarity between MeL^a and tacn, insofar that the *bis*-complexes of both ligands show less interligand repulsion than the cyclohexane-based family. For MeL^a, this effect is even more pronounced than for tacn, and as a consequence, the ratio $\beta_{120}/(\beta_{110})^2 = K_2/K_1$ (where K_1 and K_2 denote the individual formation constants of [M(MeL^a)]²⁺ and [M(MeL^a)₂]²⁺) is unusually high. This has previously already been observed for the parent L^a and results in a considerable amount of ML₂ formation in solution where total M and total L are applied in a 1:1 ratio.¹⁰

The answer to the above posed question is, however, no, if the efficacy of these triamines in metal binding is considered.

(60) Although the course in stability is predicted correctly for the different complexes in a *qualitative* manner, the calculated values ΔE^1 , ΔE^2 , and ΔE^3 do not correlate quantitatively with corresponding ΔG values ($= -RT \ln \beta$). Some reasons for this finding are obvious: The calculations have all been performed for Co^{III} and ionic size effects have not been considered. Entropic contributions and solvation effects have also not been taken into account. We became, however, also aware that the computer program MOMECC97³² appears to generally underestimate 1,3-diaxial repulsion energies in multiply substituted cyclohexanes. As a result the pre-strain effect for the tach/Me₃tach couple is probably even larger than derived from the data listed in Table 8.

Me₃tach and tacn represent very efficient metal receptors, whereas MeL^a (and even more pronounced L^a) do not. The reason is obviously the large amount of torsional strain which is generated upon complex formation with L^a and MeL^a. Inspection of Table 8 shows, that in comparison to the cyclohexane-based systems, the tacn complexes also exhibit a considerable amount of torsional strain. However, contrary to L^a and MeL^a this strain is to a considerable amount already present in the free ligand,⁵⁵ and does therefore not oppose complex formation. Similarly, *mono*-complexes of Me₃tach show a relatively high amount of unfavorable non-bonding interactions which is again already preformed in the free ligand.

As a conclusion, L^a and MeL^a are relatively poor metal binding triamines, and metal complexes with a tridentate coordination mode must be regarded as strained. Some of this strain can be released by the detachment of one of the endocyclic (secondary) amino groups, and consequently, L^a and MeL^a have a rather high tendency to coordinate in a bidentate fashion and to form protonated species. This is different for Me₃tach and tacn which form low strained structures in their tridentate coordination. Consequently, Me₃tach and tacn display mainly an all-or-nothing behavior. With regard to the currently discussed applications of such systems in catalysis and modeling of bioinorganic systems,^{8,9} we believe that it could well be of importance to be aware of these differences.

Acknowledgment. C, H, N analyses were performed by Anton Zaszka, X-ray data were collected by Dr. Volker Huch (both Universität des Saarlandes). A part of the potentiometric and spectrophotometric measurements has been performed by Tanja Komso. Hydrogenation of 2,4,6-trimethyl-1,3,5-benzotriamine was performed by Solvias Inc. (Basel, Switzerland). Financial Support by the Deutsche Forschungsgemeinschaft DFG is gratefully acknowledged.

Supporting Information Available: Crystallographic data in CIF format. Tables S1–S6 list structural parameters of M-(tacn)₂ complexes as obtained from the Cambridge Structural Data Base, the hydrogen bonding interactions in (H₃MeL^a)-(BiCl₆)·2H₂O and (H₃MeL^a)(ClO₄)Cl₂, UV/vis data of Co^{III} complexes, formation constants of Ni^{II}- and Cu^{II}-MeL^a complexes in 1 M KCl and 1 M KNO₃, formation constants of mixed Cu^{II}- and Cd^{II}-chloro-MeL^a- complexes, explicit values of the formation constants used in the linear free energy relations (eqs 1 and 2). Figures S1–S6 display packing schemes of (H₃MeL^a)-(BiCl₆)·2H₂O and (H₃MeL^a)(ClO₄)Cl₂, an NMR titration curve of (H_xMeL^a)^{x+}, ORTEP views of the molecular structure of **3**³⁺ and **5**²⁺, measured and calculated Vis spectra for Cu^{II}- and Ni^{II}-MeL^a complexes, and species distribution plots for the Cd^{II}-MeL^a- and Cd^{II}-MeL^a-Cl⁻-system. Two complements to the experimental part list additional parameters of the potentiometric and spectrophotometric measurements. This material is available free of charge via the Internet at <http://pubs.acs.org>.